bioRxiv preprint doi: https://doi.org/10.1101/2025.09.24.678321; this version posted September 26, 2025. The copyright holder for this preprint (which was not certified by peer review) is the author/funder, who has granted bioRxiv a license to display the preprint in perpetuity. It is made available under a CC-BY 4.0 International license.

Arabidopsis arenosa influences its microbiome as a serpentine soil adaptation strategy

Anita Bollmann-Giolai[1,2], Michael Giolai[1,3], Mellieha Allen[4], Darren Heavens[5], Veronika Lipánová[6], Mark Alston[5], James Brown[1], Matthew D. Clark[7], Paulina Flis[8], Filip Kolář[9], Levi Yant[8], Jacob Malone[1,10]

1) John Innes Centre, Norwich Research Park, Norwich NR4 7UH, United Kingdom

2) Max Planck Institute for Biology, Tübingen, 72076, Germany

3) Research Centre for Ecological Change, Organismal and Evolutionary Biology Research Program, Faculty of Biological and Environmental Sciences, University of Helsinki, Finland

4) Royal Botanic Gardens, Kew, Kew Green, Richmond, Surrey, TW9 3AE, United Kingdom

5) Earlham Institute, Norwich Research Park, Norwich, NR4 7UZ, United Kingdom

6) Institute of Integrative Biology, ETH Zurich, Universitätstrasse 16, 8092 Zürich, Switzerland

7) Natural History Museum, London, SW7 5BD, United Kingdom

8) University of Nottingham, Nottingham NG7 2RD, UK

9) Institute of Botany, Czech Academy of Sciences, Průhonice 252 43, Czech Republic

10) School of Biological Sciences, University of East Anglia, Norwich NR4 7TJ, United Kingdom

Correspondence

All correspondence should be issued to: jacob.malone@jic.ac.uk.

Competing Interests

The authors declare no competing interests.

Abstract

There is growing evidence that microbes can facilitate plant growth in metal-rich soils. However, our current understanding of how plants recruit their microbiomes under abiotic stress remains incomplete. Serpentine soils are elementally skewed, with high concentrations of magnesium and nickel, often accompanied by other heavy metals, which can limit calcium availability and present unique challenges to plant growth. These soils are also nutrient-poor, prone to erosion, and have low water-holding capacity. To date, the mechanisms by which plants adapt to serpentine soils remain

bioRxiv preprint doi: https://doi.org/10.1101/2025.09.24.678321; this version posted September 26, 2025. The copyright holder for this preprint (which was not certified by peer review) is the author/funder, who has granted bioRxiv a license to display the preprint in perpetuity. It is made available under a CC-BY 4.0 International license.

poorly understood and the role of plant-associated microbiomes in this process has not been described. Here, we focus on *Arabidopsis arenosa* populations adapted to serpentine conditions and investigate their bacterial and fungal microbiomes to better understand the role of plant-associated microbes in serpentine adaptation. We show that serpentine soils harbour distinct plant-associated microbiomes across different plant niches and that the plant genetic background plays a key role in shaping microbial community composition. Finally, we identify serpentine-specific bacterial and fungal variants that may contribute to plant adaptation under these challenging soil conditions.

Introduction

There is growing evidence suggesting that microbes facilitate plant growth in heavy metal rich soils[1–7]. The plant microbiome influences growth, development and health[8–20]. However, knowledge of how plants attract their microbiome under abiotic stress conditions and the consequences of this for stress survival, is incomplete[9,21,22]. Stress responses such as root morphology or exudation some of can influence plant-microbe interactions[6,21–23]. Plants from highly metal-contaminated sites show distinct microbiomes compared to non-contaminated sites[24,25]. Microorganisms can be used to bioremediate contaminated mining sites[26]. A recent study describes serpentine-derived microbes improving seedling survival in serpentine soils[27].

Serpentine soils are naturally toxic to plants, globally distributed and derived from ferromagnesium-rich mantle rocks[28,29]. They are the most abundant heavy-metal soils, with elevated nickel, chromium, cobalt and high magnesium, causing low calcium/magnesium ratios and thus magnesium toxicity for plants[28–30]. Serpentine soils often lack essential nutrients[29], are often rocky, erosion- and drought-prone, with a shallow soil profile with low water-holding capacity[28,29,31]. Such high-stress conditions can have a significant impact on the ecosystem, influencing vegetation composition and leading to a high proportion of endemic species[28,29,31]. Therefore, plants growing on these sites must tolerate both drought and heavy-metals[29,31].

Serpentine site plants and their adaptation to those conditions have been studied since the 1950s[32–38]. However, in addition to the plants' inherent capacity to adapt to abiotic and biotic stress, they further rely on their microbiome to enable growth and survival in stressful conditions[8,9,39,40].

To study plant serpentine adaptation we use an autotetraploid lineage of *A. arenosa*, an outcrosser of the *Arabidopsis* genus, distributed in central and northern Europe as a model plant[33,41,42]. *A. arenosa* repeatedly adapted to serpentine soils and also grows on mining sites[41]. The plant is a facultative excluding metallophyte and also grows on non- contaminated soils[31,43,44]. For serpentine *A. arenosa* populations, genomics data suggests that genes related to the cation transport or chemical

bioRxiv preprint doi: https://doi.org/10.1101/2025.09.24.678321; this version posted September 26, 2025. The copyright holder for this preprint (which was not certified by peer review) is the author/funder, who has granted bioRxiv a license to display the preprint in perpetuity. It is made available under a CC-BY 4.0 International license.

homeostasis are under positive selection[33,37] while a reciprocal transplant experiment documented the fitness advantage of originally serpentine plants in their native substrate[37,38]. Thus, replicated populations, fitness phenotypes and genomic selection signatures make *A. arenosa* to a suitable for serpentine adaptation[45].

Both environmental and genetic factors influence microbiome formation, but their relative roles under abiotic stress remain unclear. To address this, we examine microbiomes of serpentine and non-serpentine *A. arenosa* populations and assess the relative contributions of environment and plant genome to microbial recruitment We select populations in Austria and the Czech Republic previously characterised for serpentine adaptation[33,37]. Over two seasons, we sampled three serpentine and three nearby non-serpentine sites for microbiomes from different plant niches (i.e., leaf, root, rhizosphere and bulk soil). We also conducted a common garden transplant experiment with all six populations to test genetic effects on microbiome assemblage in both soils. We show that serpentine soils shape microbiomes across niches and that plant genetic background is a major driver of composition. We further identify serpentine-specific bacterial and fungal amplicon sequence variants (ASVs) potentially facilitating adaptation to these challenging soils.

Results

Soil ion profiles distinguish serpentine and non-serpentine sites

Serpentine soils are characterized by drought conditions, low nutrient availability, high concentrations of heavy metals and magnesium, and low levels of calcium[46,47]. Magnesium, although being essential to plant growth, has been described to exacerbate the toxicity of other ions, including heavy metals, particularly under low calcium availability[29,48,49]. As a consequence, together with heavy metals, this enhances the toxicity of serpentine soils for plants[50]. Not many plant species grow in such challenging conditions, but *A. arenosa* populations have been previously described to show local adaptation to serpentine soils[37,38,45] (**Fig. 1A**).

We selected three pairs of populations established in either serpentine or non-serpentine soils, which are growing in spatial proximity in Austria and the Czech Republic (**Fig. 1A**). To confirm the soil ion profiles of the selected sites we collected soil material along with microbiome sampling and analysed the ion composition data of all sites (**Fig. 1B-E, Extended Data File 1**). Principal component analysis (PCA) of soil ion composition showed that that serpentine and non-serpentine soils separated well along PC1, which explained 43.2 % of variance (**Fig. 1B**). Magnesium, calcium and rubidium as well as the heavy metals nickel, chromium and cobalt contributed most to the separation (**Fig. 1C**). The magnesium concentration showed the strongest association with serpentine soils along PC1. We also

bioRxiv preprint doi: https://doi.org/10.1101/2025.09.24.678321; this version posted September 26, 2025. The copyright holder for this preprint (which was not certified by peer review) is the author/funder, who has granted bioRxiv a license to display the preprint in perpetuity. It is made available under a CC-BY 4.0 International license.

analysed the Ca/Mg ratio and found that the ratio was consistently lower in serpentine than non-serpentine soils (**Fig. 1C-E**, **Extended Data File 1**). This pattern agrees with previously described characteristics of serpentine soils[32].

Microbiome community structure across serpentine and non-serpentine niches

We collected bulk soil (adjacent to plants), rhizosphere, root and leaf material in spring and fall 2018 from five plants per population. We constructed and sequenced 16S and ITS Illumina amplicon libraries and assigned ASVs[23,51], removing ASVs below a total relative abundance of 0.1%. We performed a redundancy analysis (RDA) to assess community structure across all niches using genus-level taxonomic resolution (**Fig. 2, Extended Data File 2**). Here, we observed stronger niche differentiation in bacterial communities (**Fig. 2A, Extended Data File 2**) compared to fungal communities (**Fig. 2C, Extended Data File 2**). In both bacteria and fungi, leaf-associated communities were clearly distinct from those in bulk soil, rhizosphere, and roots (**Extended Data File 2**).

ASVs were grouped by phylum and illustrated in bar plots to understand bacterial and fungal microbiome composition across populations and seasons (**Fig. 2B,D**). Bar plots indicated that the phylum-level composition of bacterial and fungal communities was largely similar between serpentine and non-serpentine sites, but showed niche specific differences between bacteria and fungi. Multiple bacterial phyla were present across all four niches, whereas fungal communities were dominated by few highly abundant phyla. This aligns with previous findings that bacterial niches exhibit greater diversity and niche differentiation compared to fungi[52]. For bacteria, 11 and 13 phyla were detected in bulk soil and rhizosphere compared to 8 in roots and 5 in leaves (**Fig. 2B**). In the bulk soil compartment Cyanobacteria, Proteobacteria, Actinobacteria, Verrumicrobiota and Acidobacteriota shared equal relative abundances (22.71 % - 16.12 % of assigned ASVs respectively). The same pattern was observed for the rhizosphere, with some changes in abundances and an increase of Cyanobacteria from 22.71 % to 31.35 % of assigned ASVs. Roots were dominated by Actinobacteria (44.19 %) and Proteobacteria (31.59 %), whereas leaves were highly enriched in Proteobacteria with 78.22 % of assigned ASVs (**Extended Data File 3**). This indicates potential niche specific shifts and composition of bacterial taxa from bulk soil to the rhizosphere, as well as roots to leaves. Fungal communities exhibited less clear niche differences (**Fig. 2D**). Bulk soil and rhizosphere contained 3 and 4 phyla while roots and leaves contained 3 and 2 phyla respectively. Ascomycota and Basidiomycota together accounted for the majority of relative abundances across all niches. Ascomycota enriched for an average percentage of 58.74 %, 56.16 %, 71.37 % and 60.26 % from bulk soil, rhizosphere, roots to leaves. For Basidiomycota these loads were 39.67 %, 41.55 %, 27.2 % and 39.24 % respectively

bioRxiv preprint doi: https://doi.org/10.1101/2025.09.24.678321; this version posted September 26, 2025. The copyright holder for this preprint (which was not certified by peer review) is the author/funder, who has granted bioRxiv a license to display the preprint in perpetuity. It is made available under a CC-BY 4.0 International license.

(**Extended Data File 3**). The observation of differences in microbial composition between niches of serpentine and non-serpentine plants agrees with previous findings by Botha *et al.*[53].

Differential abundance analysis reveals serpentine-specific enrichment of microbial taxa

We hypothesised that functional effects of a potential microbiome facilitated serpentine adaptation likely occur at a finer taxonomic resolution than the phylum level (e.g., genus or species)[53,54].

Therefore, we tested whether individual ASVs influenced differences in community composition by examining their occurrence across plants and populations: ASVs present in all populations were considered conserved, those found in two of three populations were classed as shared, and those restricted to a single population as unique (**Fig. 3A**). Analyses were performed for each niche, for serpentine and non-serpentine sites, and for bacterial and fungal communities. Across 14,021 bacterial and 5,672 fungal ASVs we found that most bacterial and fungal ASVs were unique to individual populations (**Fig. 3A, Extended Data File 4**). A fraction of 1.10 % – 9.17 % of serpentine bacterial ASVs and 7.49 % - 9.51 % for serpentine fungal ASVs was conserved across niches. For non-serpentine niches these numbers were lower with 0.31 % - 7.48 % and 3.16 % - 8.52 % for bacterial and fungal ASVs across niches respectively. We observed the highest number of conserved ASVs for fungal serpentine microbiomes (**Fig. 3A, Extended Data File 4**). Despite the large number of ASVs that were unique to individual populations, the results indicate that plants growing on serpentines harbour a conserved subset within their microbial communities that potentially contributes to serpentine adaptation[24,25,53].

To test whether these patterns reflect statistically significant compositional shifts between serpentines and non-serpentines, we performed differential abundance analysis using the microbiomeMarker package[55] (**Fig. 3B**). A total of 13,895 bacterial and 5,618 fungal ASVs met prevalence criteria[55]. Of these we found that 13.74 % of bacterial and 22.59 % of fungal ASVs were statistically significantly enriched (**Extended Data File 5, Extended Data File 6**). Whereas 2.84 % of 13.74 % of bacterial ASVs across all niches enriched for serpentines. For the fungi this pattern was the other way around and the majority of ASVs enriched for serpentines with 16.02 % of 22.59 %. These results indicate that fine-scale taxonomic shifts accompany the previously observed broader community differences. We next analysed the genera to which serpentine-enriched ASVs belonged. For each genus, we counted the number of ASVs and calculated the $\log_2$-fold-ratio of serpentine to non-serpentine ASVs. (**Extended Data File 5, Extended Data File 6**). For bacteria in bulk soil, no genus showed a substantially higher number of ASVs in serpentine sites. In the serpentine rhizosphere, *Candidatus Udaeobacter* was the most enriched genus with 47 ASVs compared to none in non-serpentine sites, followed by *Vicinamibacterales* with 16 vs. 0 ASVs. In roots, genera generally had

bioRxiv preprint doi: https://doi.org/10.1101/2025.09.24.678321; this version posted September 26, 2025. The copyright holder for this preprint (which was not certified by peer review) is the author/funder, who has granted bioRxiv a license to display the preprint in perpetuity. It is made available under a CC-BY 4.0 International license.

lower ASV numbers, with *Streptomyces* showing 4 vs. 0 ASVs compared to serpentine sites. In leaves, *Hymenobacter* and *Methylobacterium–Methylorubrum* counted more ASVs for serpentines, with 45 vs. 0 and 25 versus 0 ASVs to non-serpentines, respectively. For fungi, *Mytilinidion* (19 vs. 0), *Knufia* and *Russula* (both 13 vs. 0) were most abundant in bulk soil, while no genera were notably enriched in the rhizosphere. In roots, *Penicillium* (7 vs. 0), *Knufia*, *Sebacina,* and *Tomentella* (all 4 vs. 0) were enriched, and in leaves, *Fellozyma* was observed with 4 vs. 0 ASVs compared to non-serpentines (**Extended Data File 7**). Consolidating known literature about these genera we found commonalities among bacteria and fungi that potentially contribute to microbiome mediated serpentine adaptation. I.e., *Streptomyces* and *Methylobacterium–Methylorubrum* bacterial genera have been described to be beneficial for plant performance and growth[56–58]. *Sebacinales* fungi are potential plant growth promoting endophytes[59]. *Penicillium* fungi are described as decomposers of organic materials[60], and *Tomentella* and *Russula* have been recognised as ectomycorrhizal fungi that are important in nutrient cycling[61,62]. Hence, bacterial and fungal genera could together contribute to serpentine adaptation by facilitating nutrient availability and promoting plant growth in serpentines. This agrees with previous findings where serpentine plants have been described to associate with arbuscular mycorrhizal assemblages[63].

Serpentine microbiomes are better retained by native plants under reverse-transplant conditions

Previous studies have shown that plant genotypes can influence the composition of their associated microbiomes[64–67]. However, environmental factors also significantly impact microbial community composition and environmental stressors can influence the recruitment of specific microbial taxa that may aid in plant adaptation[68]. It remains unclear to what extent plants actively recruit microbes or whether observed effects are environmentally driven.

To examine potential recruitment effects, we predicted that non-serpentine genotypes, which are not typically adapted to serpentine soils[38], would exhibit different responses compared to serpentine genotypes under serpentine conditions. To test this, we performed a reciprocal transplant experiment in which serpentine and non-serpentine populations were grown in both serpentine and non-serpentine soils. As in the field experiment, we collected five plants for each condition, performed 16S and ITS Illumina sequencing and called ASVs[69]. We then compared ASV abundances of serpentine and non-serpentine populations grown in their native soil type with those in the transplanted (i.e., non-native) soil using Bray-Curtis similarity (**Fig. 4A,B**). We observed that microbiomes between native and non-native conditions differed substantially, yet not completely, between populations. Fungal microbiomes were more similar than bacterial microbiomes in the bulk soil and the root compartments (**Fig. 4C, Extended Data File 8**). To test whether serpentine and non-serpentine plants

bioRxiv preprint doi: https://doi.org/10.1101/2025.09.24.678321; this version posted September 26, 2025. The copyright holder for this preprint (which was not certified by peer review) is the author/funder, who has granted bioRxiv a license to display the preprint in perpetuity. It is made available under a CC-BY 4.0 International license.

recruit similar microbiomes under serpentine conditions, we compared the log_2 fold-changes of ASVs observed in the field with those measured in the transplant experiment, focusing on serpentine-to-non-serpentine enrichment. Log_2 fold-change values were compared using Spearman's rank correlation coefficients (**Fig. 4C**). The analyses showed that log_2 fold-changes in serpentine plants from the transplant experiment agreed more closely with field data and preserved the patterns observed in the field better than those of non-serpentine plants. For serpentine plants, Spearman correlation coefficients with the field data were 0.71, 0.66, and 0.59 for bulk soil, rhizosphere, and root, respectively (all statistically significant: $p \leq 2x10^{-16}$, $p = 5x10^{-3}$, and $p = 5x10^{-4}$). For non-serpentine plants, correlations were weaker with 0.62 and 0.46 for bulk soil and root (bulk soil $p = 1.8x10^{-12}$, root $p = 1.9x10^{-2}$). These results indicate that serpentine plants maintained a microbiome that more closely resembles the field serpentine gradient than non-serpentine plants. No statistically significant correlations were observed in leaves, which potentially reflects aboveground effects of growth under controlled conditions rather than patterns present in the field.

We hypothesised that ASVs with a potential role in facilitating serpentine adaptation would be statistically significantly serpentine-enriched in the field and the transplant data. We therefore compared statistically significantly enriched bacterial and fungal ASVs from the field with those from the transplant experiment (**Fig. 3D**). Overall, serpentine plants showed stronger overlap with field data than non-serpentine plants. For bacteria, only three ASVs in bulk soil were serpentine-enriched in populations of non-serpentine origin, whereas populations of serpentine origin showed greater overlap, with six ASVs in bulk soil and nine in the rhizosphere. For fungi, the numbers were generally higher. In serpentine-origin plants, we observed 90 overlapping ASVs in bulk soil, one in leaf, two in the rhizosphere, and 24 in root. In contrast, non-serpentine-origin plants showed fewer overlaps, with 21 in bulk soil, none in leaf or rhizosphere, and 10 in root.

We found that fewer bacterial ASVs were enriched under serpentine conditions, whereas fungi showed a greater number of consistently enriched ASVs, both in the field and in serpentine plants during the transplant experiment. This overlap highlights fungal ASVs as potential contributors to serpentine adaptation, particularly in belowground compartments such as bulk soil, rhizosphere, and root. Among bacteria, only a single genus, *Candidatus Udaeobacter*, was enriched in both the rhizosphere and bulk soil. In contrast, we identified 73 enriched associations with fungal taxa, 55 of which could be assigned at the genus level (the remainder assigned at higher taxonomic ranks such as phylum, order, or class). We also quantified the number of ASVs per genus and, consistent with the field data, observed overlap with genera already detected in the natural serpentine community (**Extended Data File 9**). For example, we identified six ASVs in *Penicillium*, three in *Russula*, and one each in *Mytilinidion* and *Tomentella*. Consolidating literature further we also detected the fungal

bioRxiv preprint doi: https://doi.org/10.1101/2025.09.24.678321; this version posted September 26, 2025. The copyright holder for this preprint (which was not certified by peer review) is the author/funder, who has granted bioRxiv a license to display the preprint in perpetuity. It is made available under a CC-BY 4.0 International license.

genus *Exophiala*, which has been described to promote plant growth under nickel stress, a major separator of serpentine conditions in our PCA[70] We also found the fungal genus *Phialocephala*, which is a plant growth promoter by enabling nutrient availability[71]. Previous work has shown that serpentine plants associate with distinct arbuscular mycorrhizal assemblages that may help mitigate metal stress[63]. Our findings therefore indicate potential new fungal partners involved in serpentine stress adaptation. Moreover, fungi associated with serpentine plants are often highly diverse and may include specialized taxa that confer advantages to plants growing under serpentine conditions[72,73].

Plant genotype is a stronger factor shaping microbial communities, compared to the environment

The extent to which plant-associated microbiomes are actively recruited by the host, shaped by environmental conditions, or both remains unclear[74]. Considering enrichment patterns and population differences between our field and transplant experiment, we concluded that microbiome assembly results from a complex interplay between plant genotype and environmental factors, with both likely contributing[75,76]. Disentangling the relative role of plant host and environment is essential to determine whether microbiome-mediated stress adaptation is genetically encoded and thus potentially subject to evolution or primarily environmentally induced.

To disentangle the effects of host genotype and environment on microbiome recruitment, we focused on the statistically significant, differentially enriched ASVs identified in the field experiment. Genotype data from populations revealed clear population separation in MDS analyses of k-mers from both individual genome sequencing[37] (**Extended Data File 2**). We then applied generalized linear mixed models (GLMMs) to test whether ASV abundances were explained by environment (serpentine vs. non-serpentine), genotype (population), or their interaction. Model contributions were quantified using R^2 values. Across all four niches, the combined effect of genotype and environment accounted for the largest proportion of variance. Importantly, for both bacterial and fungal communities, genotype-only models consistently explained more variance than environment-only models. These results indicate that microbiome assembly is shaped by both host genotype and environment, with a stronger contribution from genotype (**Fig. 5**). This pattern supports the idea that serpentine adaptation reflects a long-term evolutionary process involving both plants and their associated microbiomes.

Discussion

In this study, we conducted an in-depth examination of the microbiome communities associated with *A. arenosa* plants growing in the challenging environment of serpentine soils. Serpentine soils impose multiple simultaneous stresses, including low calcium-to-magnesium ratios, high heavy metal loads,

bioRxiv preprint doi: https://doi.org/10.1101/2025.09.24.678321; this version posted September 26, 2025. The copyright holder for this preprint (which was not certified by peer review) is the author/funder, who has granted bioRxiv a license to display the preprint in perpetuity. It is made available under a CC-BY 4.0 International license.

and nutrient deficiencies[32]. We show that serpentine soils differ from non-serpentine soils in their ionomic composition, most notably by a lower calcium-to-magnesium ratio. We further demonstrate that microbiomes of serpentine and non-serpentine plant populations differ in both bacterial and fungal composition across all tested compartments, from bulk soil to rhizosphere, roots, and leaves. In a reciprocal transplant experiment, exposing plants of serpentine and non-serpentine origin to both their native and non-native soils, we observe distinct microbial compositions depending on plant origin and soil type.

By carefully confirming field observations with a transplant experiment, we identify several ASVs and genera that can contribute to microbiome-mediated serpentine adaptation. Notably, many of the genera that we find as statistically significantly associated with serpentine soils are described to enhance either nutrient availability or to promote plant growth. This involves the coordinated contribution of both bacteria and fungi. Beneficial bacterial genera that we identify, such as *Streptomyces* and *Methylobacterium–Methylorubrum* enhance plant growth[56–58], while fungal taxa including *Sebacinales*, *Penicillium*, *Tomentella*, and *Russula* support nutrient cycling, organic matter decomposition, and soil nutrient acquisition[59–62]. Additionally, *Exophiala* and *Phialocephala* promote plant growth under nickel stress and improve nutrient availability[70,71]. Together, these microbes likely facilitate plant survival and growth under serpentine stress, complementing known associations with arbuscular mycorrhizal fungi[63]. Considering that serpentine soils are nutrient-poor and subject to heavy metal stress[32,46,47], the coordinated presence of microbial taxa that enhance nutrient availability, promote plant growth, and mitigate metal stress is likely crucial for plant survival under these conditions[9]. From an ecological and evolutionary perspective, these results are particularly impactful because they demonstrate a potential mechanism by which plants can extend their adaptive capacity through microbial partnerships.

In previous findings Konečná *et al.*[37] reported that *A. arenosa* exhibits an adaptive phenotype in serpentine soils, with this adaptation linked to 60 candidate genes, notably including the calcium channel *TPC1*. Whereas *TPC1* has not been connected to microbiome recruitment in detail[37], calcium channels play a role in plant signaling, microbe interactions[77]. In addition to confirming the importance of plant genetics in serpentine adaptation, we further show that the host genotype exerts a stronger effect than soil environment on the microbiome composition. This suggests that heritable plant traits influence microbial recruitment in ways that could reinforce adaptive phenotypes under stressful conditions. Such findings provide direct evidence supporting the holobiont concept, in which the plant and its microbiome function as an integrated adaptive unit[39]. Recognising the plant and its microbiome as an integrated adaptive unit opens new avenues for research and provides a roadmap for sustainable strategies to enhance plant health and productivity in challenging ecosystems[74,76,78,79].

bioRxiv preprint doi: https://doi.org/10.1101/2025.09.24.678321; this version posted September 26, 2025. The copyright holder for this preprint (which was not certified by peer review) is the author/funder, who has granted bioRxiv a license to display the preprint in perpetuity. It is made available under a CC-BY 4.0 International license.

In conclusion, our work highlights that microbial contributions to plant adaptation are both specific and compartmentalized. The distinct patterns observed across niches demonstrate that adaptive microbiomes are not uniform, but finely tuned to plant physiology and environmental context, indicating tight plant–microbe co-evolution. This nuance is critical for understanding microbiome-mediated stress adaptation, which cannot be inferred solely from bulk soil or aboveground sampling.

Our results bridge mechanistic understanding of plant adaptation with applied significance. Serpentine soils can serve as a natural testbed to identify microbial taxa and plant genes that contribute to stress resilience. Understanding which plant loci drive microbial recruitment could allow future strategies to engineer crops that actively recruit beneficial microbes under nutrient-poor or metal-contaminated conditions. This moves beyond correlative microbiome studies: it suggests a pathway for predictive microbiome management, where plant genotype informs the assembly of adaptive microbial consortia.

Online Methods

Field sampling collection-strategy

Serpentine and nearby, genetically close non-serpentine control populations were collected in the Czech Republic and in Austria (**Fig. 1**). Populations N1 (49.734963, 15.174846, Vlastejovice) and S1 (49.683816, 15.133256, Borovsko) are located in the Czech Republic. Populations S2 (48.629930, 15.542567, Steinegg) and N2 (48.631497, 15.557237, Fuglau) are in Lower Austria, Austria and S3 (47.281679, 14.927647, Gulsen) and N3 (47.284170, 14.681940, Ingeringgraben) are in Styria, Austria. The selected populations were sampled in spring 2018 and fall 2018. For each population different tissues were sampled for their microbiomes: 1) leaf endophytes with closely associated epiphytes, 2) root endophytes with closely associated epiphytes, 3) rhizosphere and nearby 4) bulk soil. As microbial communities can change over time[80,81], we sampled all tissues at each time-point. For this, leaves, roots, rhizosphere and bulk soil were collected in ten replicates. Additionally, soil and leaf material were collected for comprehensive ionomic profiling at each time point.

Field sample collection – microbiome samples

All plant and soil material were collected using previously sterilised nitrile gloves and stored in 2 ml Eppendorf safe-lock tubes (Eppendorf) in RNAlater (SIGMA-ALDRICH) to minimise microbial gDNA degradation and community shifts. The sampled material was stored in a mobile refrigerator during transportation where the material was stored at -80 °C until use for gDNA extraction.

Field sample collection – microbiome samples of transplant experiment

bioRxiv preprint doi: https://doi.org/10.1101/2025.09.24.678321; this version posted September 26, 2025. The copyright holder for this preprint (which was not certified by peer review) is the author/funder, who has granted bioRxiv a license to display the preprint in perpetuity. It is made available under a CC-BY 4.0 International license.

The transplant experiment is already published and described in[37,38]. In brief, to investigate adaptation mechanisms of serpentine populations of *A. arenosa* to serpentine soils Konečná et al grew each serpentine and its non-serpentine control population in a common garden set up in the experimental garden of the Charles University, Prague (Czech Republic) over the growing season of 2019. Each serpentine population was grown in its native serpentine soil and in the soil of its paired control non-serpentine population and vice versa. Specifically, serpentine populations (S1, S2, S3) were grown in their own serpentine soils (S1, S2, S3) as well as in the corresponding non-serpentine soils (N1, N2, N3). Likewise, non-serpentine populations (N1, N2, N3) were grown in their own soils and in the paired serpentine soils (S1, S2, S3). For example, population S1 was grown in its native serpentine S1 soil and in the paired non-serpentine N1 soil, and population N1 was grown in its native N1 soil and the paired serpentine S1 soil. In total 284 plants have been grown in total for the six populations, with 44-50 plants per population[37].

To investigate the role of the plant microbiome in serpentine soil adaptation, leaf, root and bulk-soil material was collected for all populations grown in their natural and non-natural condition. All samples had been collected in September 2019 with five replicates per plant tissue, population and treatment. The collection and storing process was conducted as described above for microbiome samples.

Field sample collection – ionomic profiling material

Soil and leaf material were collected for ionomic elemental profiling. The soil was collected into 15 ml conical tubes (Supplier Starlab (UK) Ltd). Leaves were collected into tea bags and stored in a box containing silica gel to reduce moisture. The material was stored at room temperature until preparation for elemental profiling.

Ionomic material preparation

The leaf and soil material were prepared for ionomic profiling by air-drying the soil for a minimum of one week on the bench at room temperature and baking the leaves for three days at 60˚C until the material was dry. The soil material was additionally sieved after baking to remove any debris. Leaf and soil samples underwent elemental profiling with Inductively Coupled Plasma Mass Spectrometry (ICP-MS) similar as described in[33,82]. Profiled elements were (names according to periodic table annotations): Ca, Mg, Mn, Ni, Cr, Rb, Co and Fe.

Ion profile analyses

Ion concentration for elements of interest (namely Ca, Mg, Mn, Ni, Cr, Rb, Co and Fe) were visualised using custom scripts in R-4.4.1 with the ggplot2-3.5.1 package[83]. Statistic differences between serpentine and non-serpentine sites were tested using the stat_compare_means package of ggpubr-

bioRxiv preprint doi: https://doi.org/10.1101/2025.09.24.678321; this version posted September 26, 2025. The copyright holder for this preprint (which was not certified by peer review) is the author/funder, who has granted bioRxiv a license to display the preprint in perpetuity. It is made available under a CC-BY 4.0 International license.

0.6.0[84], specifying Wilcoxon rank-sum testing. The principal component analysis (PCA) was performed using the default R-4.4.1 prcomp function. The graph of variables was visualised using the fviz_pca_var function of factoextra-1.0.7[85] with default settings and the ggplot2-3.5.1[83] package in R-4.4.1.

Map of populations

Geographic coordinates of the serpentine and non-serpentine populations were converted into spatial features using the sf-1.0 package in R-4.4.1, with WGS84 (EPSG:4326) as the reference coordinate system. For visualization, a base map of Austria and Czechia was obtained from the rnaturalearth-1.0.0 package at medium scale and used to display the location of populations[86] with ggplot2-3.5.1[83].

Microbiome sample preparation

Samples were stored in RNAlater[82,87–90]. Roots and leaves were transferred into a fresh 2 ml tube and washed with 2 ml 0.1 M potassium phosphate pH 8.0 buffer with shaking at 200 rpm for 30 min. Afterwards the root was transferred into a fresh 2 ml tube and supernatant was retained as the rhizosphere sample. This step was repeated three times, with fresh buffer each time. Afterwards the sample was vortexed twice for 30 seconds with fresh 2 ml 0.1 M potassium phosphate pH 8.0 buffer and the root was transferred into a fresh 2 ml tube. The supernatant was added to the previously collected supernatant. The combined supernatant was centrifuged for 10 min with 15,000 rcf and room temperature. After removing the supernatant, the pellet was kept as a rhizosphere sample and stored at -80˚C until further use. Leaf samples were washed with 2 ml 0.1 M potassium phosphate pH 8.0 buffer by vortexing twice for 10 sec. This step was repeated three times. The supernatant was decanted, and leaves transferred into a fresh 2 ml tube and stored at -80˚C until further use.

Microbiome gDNA extraction of field and transplant experiment samples

The gDNA extraction for the field and common garden experiment was performed as described by Bollmann-Giolai *et al.*[51] using 250 mg soil, before gDNA was purified in a 96-well format from 140 µl supernatant using magnetic beads (Sera-Mag Carboxylate-Modified Magnetic Particles (Hydrophophilic), GE Healthcare Life Sciences). The cleaned gDNA was transferred to a fresh 96 well plate and stored at -20 ˚C until further use.

Wet lab – Amplicon bacterial and fungal library construction

Amplicon data was analysed as previously described[23,51]. In brief: The bacterial variable (V4) region of the 16S rRNA gene and the fungal ITS1 region of the Internal Transcribed Spacer were targeted for amplicon library construction using 16S 515 forward, 16S 806 reverse, ITS 1 forward and ITS2 reverse primers adapted from Walters et al [91] (**Extended Data File 10**). Amplicon library construction was

bioRxiv preprint doi: https://doi.org/10.1101/2025.09.24.678321; this version posted September 26, 2025. The copyright holder for this preprint (which was not certified by peer review) is the author/funder, who has granted bioRxiv a license to display the preprint in perpetuity. It is made available under a CC-BY 4.0 International license.

performed using a two-step PCR protocol as previously described[23,51]: In a first PCR the 16S V4 and ITS regions were targeted using gene specific primers, followed by custom dual indexing in a barcoding PCR (**Extended Data File 10**). For the bacterial 16S V4 PCRs PNAs (peptide nucleic acid PCR clamps) were included targeting plant mitochondria (mPNA) and chloroplast regions (cPNA)[92] in the first PCR to minimise plant gene amplification. Library construction was conducted as previously described[23,51]. Briefly, the first PCR step was performed with three technical replicates using 3 ng gDNA. Samples were then pooled and subjected to a 0.7x magnetic bead clean-up (MAGBIO) and eluted in 10 µl TE buffer. The second PCR was conducted using the program for bacterial and fungal libraries previously described[23,51].

The cleaned amplicon libraries were quantified using the Qubit 2.0 fluorometer (Thermo Fisher Scientific) with dsDNA HS Assay Kit reagents (Thermo Fisher Scientific) and the size of the amplicons was controlled on the GX Touch using the 3K kit (X-Mark DNA LabChip, HT DNA NGS 3K Reagent Kit, Perkin Elmer LAS (UK) LTD). Amplicons were pooled equimolarly to 1.5 nM for bacterial and 2.0 nM for fungal libraries according to the molarity. A final 0.7 x magnetic bead clean-up (HighPrep™ PCR Clean-up System, MAGBIO) was performed and the final library pools were eluted in 50 µl EB buffer.

Sequencing on NovaSeq SP flowcell

The libraries were equimolarly pooled for NovaSeq sequencing. Prior to submission the final library pools were concentrated with a 0.7x magnetic bead clean-up and eluted in 50 µl EB buffer. The libraries were sequenced on one SP flow cell on the NovaSeq with a 30 % PhiX spike-in.

Amplicon sequence variant taxonomy assignment and filtering

Amplicon data analysis was conducted as previously described[23,51] with minor alterations: The Illumina binary base call files (bcl) were demultiplexed using bcl2fastq version 2-2.20.0.422 with the settings --barcode-mismatches 1 --fastq-compression-level 9 into individual fastq.gz files. The paired-end reads were trimmed for primers, sequencing adapters and linker sequences using cutadapt-1.9.1[93] with the settings -n 4 --minimum-length=50. Following cutadapt fastp-0.20.0[94] was run on 16S data with disabled length filter and trim_poly_g to trim polyG read tails. Afterwards both 16S and ITS data was quality controlled, trimmed and filtered using R-3.6.3 and DADA2 version 1.14.1 according to the workflow described in version 2[95]. The truncation length for forward reads was set to 210 bp and the truncation length for the reverse reads to 210 bp for both 16S and ITS. The truncation length was based on read quality. For 16S and ITS libraries we used the following parameters: maxN=0, maxEE=c(2, 2) and truncQ=2 and a minimum length of 50 bp. The filtering parameter maxEE chosen allows for a maximum of 2 expected errors per read, the filtering parameter maxN chosen does not

bioRxiv preprint doi: https://doi.org/10.1101/2025.09.24.678321; this version posted September 26, 2025. The copyright holder for this preprint (which was not certified by peer review) is the author/funder, who has granted bioRxiv a license to display the preprint in perpetuity. It is made available under a CC-BY 4.0 International license.

allow any Ns. In addition to filtering using maxEE, maxN and read trimming, a quality score (truncQ) was set that truncates the read at the first nucleotide with a quality score of 2 (set value). After these filtering steps, error rates were estimated as described in[95] and the data was denoised with standard inference settings[95]. Forward and reverse reads were merged with default settings: if the minimum of 12 identical bases for overlap was not met between forward and reverse reads, the sample would be omitted. Following the merging of paired reads, a sequence table was constructed with amplicon sequence variants (ASVs). As an additional, subsequent filtering step, chimaeras were removed using standard settings[95]. The Silva (silva_nr99_v138.1.train.set.fa)[96] and UNITE (sh_general_release_dynamic_all_04.04.2024.fasta)[97] databases were then used to taxonomically classify bacterial and fungal reads respectively. Reads that did not match either the bacterial or fungal database were removed.

Amplicon sequence variants (ASVs) were used to classify both bacterial and fungal reads. A minimum read number after filtering of 1000 reads per sample and a minimum of three samples per dataset was set as cut-off. We further applied a hard-filter removing all ASVs which were not supported by at least 10 reads per sample and a total relative abundance of 0.1 %. Filtering reduced the number of reads in our 16S libraries from an initial average of 177,387 raw reads to 42,854 reads per library after filtering and assignment to ASVs. For ITS libraries, we initially obtained an average of 77,998 raw reads, which was reduced to 65,666 reads per library following taxonomic assignment. After quality controlling, trimming, taxon assignments and filtering, which were all carried out on the Norwich high-performance computing cluster, we continued with analyses on a desktop machine in R-4.4.1.

Alpha- and beta-diversity comparisons

Alpha-diversity (Shannon and Observed measures) was calculated on pre-normalised data using the phyloseq-1.48.0 package[98]. Statistical significance of diversity differences was assessed with Kruskal-Wallis rank sum tests and pairwise Wilcoxon rank sum tests for non-normally distributed data, or with ANOVA followed by Tukey's HSD for normally distributed data, using default functions in R-4.4.1.

For beta-diversity analysis, read counts were transformed using the transform_sample_counts function of phyloseq-1.48.0[98]. Bray-Curtis dissimilarities were calculated with the vegan-2.6 package in R-4.4.1 and community-level differences were tested using ANOSIM and PERMANOVA (adonis function) with the vegan-2.6 package[99]. To visually assess differences between niches we visualised samples using RDA plots in R-4.4.1 and custom ggplot2-3.5.1[83].

Relative abundance plots across niches and conditions

bioRxiv preprint doi: https://doi.org/10.1101/2025.09.24.678321; this version posted September 26, 2025. The copyright holder for this preprint (which was not certified by peer review) is the author/funder, who has granted bioRxiv a license to display the preprint in perpetuity. It is made available under a CC-BY 4.0 International license.

To show relative abundance plots of phyla across plant niches, we used custom R-4.4.1 scrips. We agglomerated taxa to phyla using the phyloseq-1.48.0[98] tax_glom function and visualised relative abundances per phylum as percent-of-all ASVs using ggplot2-3.5.1[83].

Calculating sharedness of ASVs

The sharedness of microbial ASVs between serpentine or non-serpentine populations were calculated using custom R-4.4.1 scripts. ASVs that were found in all each of three serpentine or non-serpentine populations were assigned to the conserved group. ASVs present in two populations were assigned to the shared group. ASVs present in only one population were annotated as unique. The data were visualised using ggplot2-3.5.1[83] in R-4.4.1.

Differential abundance testing of ASVs

Differential abundance (i.e., enrichment) testing between serpentine and non-serpentine conditions for each niche was performed using the default microbiomeMarker-1.10.0[55] settings with its run_limma_voom and marker_table functions in R-4.4.1. Enrichment tables were expanded by connecting ASVs with their taxonomy using custom R-4.4.1 scripts and visualised the data either as a volcano-plot or scatterplots comparing adjusted p-values using custom ggplot2-3.5.1[83]. The comparison between field and transplant enrichment (i.e., log2 fold-change values obtained by the run_limma_voom) function was visualised using ggplot2-3.5.1[83]. Spearman's correlation coefficients were calculated using the stat_cor function of ggpubr-0.6.0[84] in R-4.4.1.

Bray-Curtis comparison of microbiomes

The Bray-Curtis distance of microbiomes from transplanted populations was calculated using the vegdist function of the vegan-2.6 package[99] in R-4.4.1. For each population and niche relative abundance values of genera detected under the serpentine as well as non-serpentine conditions were combined to an abundance matrix. The abundance matrix was analysed using the vegdist function. The obtained results were visualised using custom ggplot2-3.5.1 scripts.

Estimating microbial or genotype variances

To determine genotype profiles of serpentine and non-serpentine populations we compared k-mers of *A. arenosa* genomes previously collected from each population using kWIP-0.2.0[100] default settings. This produced a distance matrix, which was analysed using the default cmdscale function in R-4.4.1. The output of the Classic Multi-dimensional Scaling (MDS) analysis was visualised using ggplot2-3.5.1[83]. This resulted in distinct separation of genotypes by population on the MDS plot.

bioRxiv preprint doi: https://doi.org/10.1101/2025.09.24.678321; this version posted September 26, 2025. The copyright holder for this preprint (which was not certified by peer review) is the author/funder, who has granted bioRxiv a license to display the preprint in perpetuity. It is made available under a CC-BY 4.0 International license.

To obtain a single environmental variable describing serpentine versus non-serpentine stress across all tested elements, the previously calculated PC1 values of populations were used. These values captured variation in calcium/magnesium stress and heavy metal composition.

To estimate environmental and genotype contributions to bacterial and fungal community assembly, all ASVs that were statistically significantly enriched in the field experiment under either serpentine or non-serpentine conditions were retained. Based on the total relative abundance of each ASV, generalized linear mixed models (GLMMs) were fitted using the glmer function of the lme4-1.1[101] package in R-4.4.1. To disseminate contributions of the genotype or the environment to microbial abundance three models were tested. (1) A full model, in which microbial abundance was explained by both population identity and condition, with time included as a random effect. (2) A population-only model, in which microbial abundance was explained by population identity and time as a random effect. (3) An environment-only model, in which microbial abundance was explained by condition and time as a random effect. All models were fitted using a Gamma distribution with a log link function. Optimization was performed using a maximum number of iterations of 1e5. For each fitted model with a statistically significant contribution of genotype or environment to microbiome assembly, conditional R^2 values were calculated using r2 function of the performance-0.12.4[102] package in R-4.4.1. Model coefficients were extracted and R^2 values visualised using custom ggplot2-3.5.1 scripts.

Acknowledgements

We thank Iain Macaulay for helpful discussion about the newest genomic methodologies, Alba Pacheco-Moreno for discussions about plant-microbe interactions and David E. Salt for his support with elemental profiling.

Funding

This work was supported by the European Research Council (ERC) under the European Union's Horizon 2020 research and innovation program [grant number ERC-StG 679056 HOTSPOT], via a grant to LY. MG was funded by the BBSRC DTP Studentship Award (BB/M011216/1). MaA was funded by ERC-StG 679056 HOTSPOT. JB, MeA and JGM were supported by Biotechnology and Biological Sciences Research Council (BBSRC) Institute Strategic Programme grants BBS/E/J/000PR9797 and BB/X010996/1 to the John Innes Centre. FK and VK were supported by the European Research Council (ERC) under the European Union's Horizon 2020 research and innovation program [grant number ERC-StG 850852 DOUBLE ADAPT], via a grant to FK. ABG was supported by a John Innes Foundation Rotation PhD Studentship.

bioRxiv preprint doi: https://doi.org/10.1101/2025.09.24.678321; this version posted September 26, 2025. The copyright holder for this preprint (which was not certified by peer review) is the author/funder, who has granted bioRxiv a license to display the preprint in perpetuity. It is made available under a CC-BY 4.0 International license.

509 **Data Availability Statement**

510 The sequencing data can be accessed at the NCBI BioProject database (BioProject ID: PRJEB71077).

511 **References**

512 1. Zadel, U. *et al.* Changes induced by heavy metals in the plant-associated microbiome of
513 Miscanthus x giganteus. *Science of The Total Environment* **711**, 134433 (2020).
514 2. Mesa, J. *et al.* Endophytic Cultivable Bacteria of the Metal Bioaccumulator Spartina maritima
515 Improve Plant Growth but Not Metal Uptake in Polluted Marshes Soils. *Front Microbiol* **6**,
516 (2015).
517 3. Feng, N.-X. *et al.* Efficient phytoremediation of organic contaminants in soils using plant–
518 endophyte partnerships. *Science of The Total Environment* **583**, 352–368 (2017).
519 4. Azcón, R., Perálvarez, M. del C., Roldán, A. & Barea, J.-M. Arbuscular mycorrhizal fungi, Bacillus
520 cereus, and Candida parapsilosis from a multicontaminated soil alleviate metal toxicity in
521 plants. *Microb. Ecol.* **59**, 668–677 (2010).
522 5. Gontia-Mishra, I., Sapre, S., Sharma, A. & Tiwari, S. Alleviation of Mercury Toxicity in Wheat by
523 the Interaction of Mercury-Tolerant Plant Growth-Promoting Rhizobacteria. *J Plant Growth*
524 *Regul* **35**, 1000–1012 (2016).
525 6. Schützendübel, A. & Polle, A. Plant responses to abiotic stresses: heavy metal-induced
526 oxidative stress and protection by mycorrhization. *J Exp Bot* **53**, 1351–1365 (2002).
527 7. Cabello-Conejo, M. I. *et al.* Rhizobacterial inoculants can improve nickel phytoextraction by the
528 hyperaccumulator Alyssum pintodasilvae. *Plant Soil* **379**, 35–50 (2014).
529 8. Turner, T. R., James, E. K. & Poole, P. S. The plant microbiome. *Genome Biol.* **14**, 209 (2013).
530 9. Caddell, D. F., Deng, S. & Coleman-Derr, D. Role of the Plant Root Microbiome in Abiotic Stress
531 Tolerance. in *Seed Endophytes: Biology and Biotechnology* (eds. Verma, S. K. & White, J., James
532 Francis) 273–311 (Springer International Publishing, Cham, 2019). doi:10.1007/978-3-030-
533 10504-4_14.
534 10. Schlaeppi, K. & Bulgarelli, D. The Plant Microbiome at Work. *MPMI* **28**, 212–217 (2014).

bioRxiv preprint doi: https://doi.org/10.1101/2025.09.24.678321; this version posted September 26, 2025. The copyright holder for this preprint (which was not certified by peer review) is the author/funder, who has granted bioRxiv a license to display the preprint in perpetuity. It is made available under a CC-BY 4.0 International license.

11. Berendsen, R. L., Pieterse, C. M. J. & Bakker, P. A. H. M. The rhizosphere microbiome and plant health. *Trends in Plant Science* **17**, 478–486 (2012).

12. Xia, Y., DeBolt, S., Dreyer, J., Scott, D. & Williams, M. A. Characterization of culturable bacterial endophytes and their capacity to promote plant growth from plants grown using organic or conventional practices. *Front Plant Sci* **6**, 490 (2015).

13. Schenk, P. M., Carvalhais, L. C. & Kazan, K. Unraveling plant–microbe interactions: can multi-species transcriptomics help? *Trends in Biotechnology* **30**, 177–184 (2012).

14. Ritpitakphong, U. *et al.* The microbiome of the leaf surface of Arabidopsis protects against a fungal pathogen. *New Phytol* **210**, 1033–1043 (2016).

15. Murphy, B. R., Doohan, F. M. & Hodkinson, T. R. Fungal root endophytes of a wild barley species increase yield in a nutrient-stressed barley cultivar. *Symbiosis* **65**, 1–7 (2015).

16. Samad, A., Trognitz, F., Compant, S., Antonielli, L. & Sessitsch, A. Shared and host-specific microbiome diversity and functioning of grapevine and accompanying weed plants. *Environ Microbiol* **19**, 1407–1424 (2017).

17. Cappelletti, M. *et al.* Leaf Treatments with a Protein-Based Resistance Inducer Partially Modify Phyllosphere Microbial Communities of Grapevine. *Front. Plant Sci.* **7**, (2016).

18. Mousa, W. K. *et al.* Root-hair endophyte stacking in finger millet creates a physicochemical barrier to trap the fungal pathogen *Fusarium graminearum*. *Nature Microbiology* **1**, 16167 (2016).

19. Khalaf, E. M. & Raizada, M. N. Bacterial Seed Endophytes of Domesticated Cucurbits Antagonize Fungal and Oomycete Pathogens Including Powdery Mildew. *Front. Microbiol.* **9**, (2018).

20. Kidd, P. S., Álvarez-López, V., Becerra-Castro, C., Cabello-Conejo, M. & Prieto-Fernández, Á. Chapter Three - Potential Role of Plant-Associated Bacteria in Plant Metal Uptake and Implications in Phytotechnologies. in *Advances in Botanical Research* (eds. Cuypers, A. & Vangronsveld, J.) vol. 83 87–126 (Academic Press, 2017).

bioRxiv preprint doi: https://doi.org/10.1101/2025.09.24.678321; this version posted September 26, 2025. The copyright holder for this preprint (which was not certified by peer review) is the author/funder, who has granted bioRxiv a license to display the preprint in perpetuity. It is made available under a CC-BY 4.0 International license.

561 21. Zhalnina, K. *et al.* Dynamic root exudate chemistry and microbial substrate preferences drive
562 patterns in rhizosphere microbial community assembly. *Nat Microbiol* **3**, 470–480 (2018).
563 22. Hu, L. *et al.* Root exudate metabolites drive plant-soil feedbacks on growth and defense by
564 shaping the rhizosphere microbiota. *Nature Communications* **9**, 2738 (2018).
565 23. Pacheco-Moreno, A. *et al.* The genotype of barley cultivars influences multiple aspects of their
566 associated microbiota via differential root exudate secretion. *PLOS Biology* **22**, e3002232
567 (2024).
568 24. Corretto, E. *et al.* Complete genome sequence of the heavy metal resistant bacterium
569 Agromyces aureus AR33T and comparison with related Actinobacteria. *Stand Genomic Sci* **12**,
570 (2017).
571 25. Garaiyurrebaso, O. *et al.* Long-term effects of aided phytostabilisation on microbial
572 communities of metal-contaminated mine soil. *FEMS Microbiol Ecol* **93**, (2017).
573 26. Van Rossum, T. *et al.* Microbiome Analysis Across a Natural Copper Gradient at a Proposed
574 Northern Canadian Mine Site. *Front. Environ. Sci.* **3**, (2016).
575 27. Igwe, A. N. & Vannette, R. L. Bacterial communities differ between plant species and soil type,
576 and differentially influence seedling establishment on serpentine soils. *Plant Soil* (2019)
577 doi:10.1007/s11104-019-04135-5.
578 28. Wójcik, M. *et al.* Chapter One - Metallophytes of Serpentine and Calamine Soils – Their Unique
579 Ecophysiology and Potential for Phytoremediation. in *Advances in Botanical Research* (eds.
580 Cuypers, A. & Vangronsveld, J.) vol. 83 1–42 (Academic Press, 2017).
581 29. Brady, K. U., Kruckeberg, A. R. & Jr, H. D. B. Evolutionary Ecology of Plant Adaptation to
582 Serpentine Soils. *Annual Review of Ecology, Evolution, and Systematics* **36**, 243–266 (2005).
583 30. Bratteler, M., Lexer, C. & Widmer, A. Genetic architecture of traits associated with serpentine
584 adaptation of Silene vulgaris. *Journal of Evolutionary Biology* **19**, 1149–1156 (2006).
585 31. Bothe, H. & Słomka, A. Divergent biology of facultative heavy metal plants. *Journal of Plant*
586 *Physiology* **219**, 45–61 (2017).

bioRxiv preprint doi: https://doi.org/10.1101/2025.09.24.678321; this version posted September 26, 2025. The copyright holder for this preprint (which was not certified by peer review) is the author/funder, who has granted bioRxiv a license to display the preprint in perpetuity. It is made available under a CC-BY 4.0 International license.

587 32. Whittaker, R. H. The Ecology of Serpentine Soils. *Ecology* **35**, 258–288 (1954).

588 33. Arnold, B. J. *et al.* Borrowed alleles and convergence in serpentine adaptation. *Proc. Natl.*
589 *Acad. Sci. U.S.A.* **113**, 8320–8325 (2016).

590 34. Turner, T. L., Bourne, E. C., Von Wettberg, E. J., Hu, T. T. & Nuzhdin, S. V. Population
591 resequencing reveals local adaptation of Arabidopsis lyrata to serpentine soils. *Nat Genet* **42**,
592 260–263 (2010).

593 35. Selby, J. P. & Willis, J. H. Major QTL controls adaptation to serpentine soils in Mimulus guttatus.
594 *Molecular Ecology* **27**, 5073–5087 (2018).

595 36. Sobczyk, M. K., Smith, J. a. C., Pollard, A. J. & Filatov, D. A. Evolution of nickel
596 hyperaccumulation and serpentine adaptation in the Alyssum serpyllifolium species complex.
597 *Heredity* **118**, 31–41 (2017).

598 37. Konečná, V. *et al.* Parallel adaptation in autopolyploid Arabidopsis arenosa is dominated by
599 repeated recruitment of shared alleles. *Nat Commun* **12**, 4979 (2021).

600 38. Konečná, V. *et al.* Genomic basis and phenotypic manifestation of (non-)parallel serpentine
601 adaptation in Arabidopsis arenosa. *Evolution* **76**, 2315–2331 (2022).

602 39. Hassani, M. A., Durán, P. & Hacquard, S. Microbial interactions within the plant holobiont.
603 *Microbiome* **6**, 58 (2018).

604 40. Pascale, A., Proietti, S., Pantelides, I. S. & Stringlis, I. A. Modulation of the Root Microbiome by
605 Plant Molecules: The Basis for Targeted Disease Suppression and Plant Growth Promotion.
606 *Front. Plant Sci.* **10**, (2020).

607 41. Koch, M. A. & Matschinger, M. Evolution and genetic differentiation among relatives of
608 Arabidopsis thaliana. *Proc. Natl. Acad. Sci. U.S.A.* **104**, 6272–6277 (2007).

609 42. Clauss, M. J. & Koch, M. A. Poorly known relatives of Arabidopsis thaliana. *Trends in Plant*
610 *Science* **11**, 449–459 (2006).

bioRxiv preprint doi: https://doi.org/10.1101/2025.09.24.678321; this version posted September 26, 2025. The copyright holder for this preprint (which was not certified by peer review) is the author/funder, who has granted bioRxiv a license to display the preprint in perpetuity. It is made available under a CC-BY 4.0 International license.

611 43. Turisová, I., Štrba, T., Aschenbrenner, Š. & Andráš, P. Arabidopsis arenosa (L.) Law. on
612 metalliferous and non-metalliferous sites in central Slovakia. *Bull Environ Contam Toxicol* **91**,
613 469–474 (2013).
614 44. Preite, V. *et al.* Convergent evolution in Arabidopsis halleri and Arabidopsis arenosa on
615 calamine metalliferous soils. *bioRxiv* 459362 (2018) doi:10.1101/459362.
616 45. Konečná, V., Yant, L. & Kolář, F. The Evolutionary Genomics of Serpentine Adaptation. *Frontiers*
617 *in Plant Science* **11**, (2020).
618 46. Anacker, B. L. The nature of serpentine endemism. *Am. J. Bot.* **101**, 219–224 (2014).
619 47. Veatch-Blohm, M. E., Roche, B. M. & Dahl, E. E. Serpentine populations of Arabidopsis lyrata
620 ssp. lyrata show evidence for local adaptation in response to nickel exposure at germination
621 and during juvenile growth. *Environmental and Experimental Botany* **138**, 1–9 (2017).
622 48. Kazakou, E., Dimitrakopoulos, P. G., Baker, A. J. M., Reeves, R. D. & Troumbis, A. Y. Hypotheses,
623 mechanisms and trade-offs of tolerance and adaptation to serpentine soils: from species to
624 ecosystem level. *Biological Reviews* **83**, 495–508 (2008).
625 49. Main, J. L. Magnesium and Calcium Nutrition of a Serpentine Endemic Grass. *American Midland*
626 *Naturalist* **105**, 196 (1981).
627 50. Rengel, Z., Bose, J., Chen, Q. & Tripathi, B. N. Magnesium alleviates plant toxicity of aluminium
628 and heavy metals. *Crop Pasture Sci.* **66**, 1298 (2015).
629 51. Bollmann-Giolai, A. *et al. A Low-Cost Pipeline for Soil Microbiome Profiling*.
630 http://biorxiv.org/lookup/doi/10.1101/2020.05.07.082305 (2020)
631 doi:10.1101/2020.05.07.082305.
632 52. Malard, L. A. *et al.* Comparative analysis of diversity and environmental niches of soil bacterial,
633 archaeal, fungal and protist communities reveal niche divergences along environmental
634 gradients in the Alps. *Soil Biology and Biochemistry* **169**, 108674 (2022).

bioRxiv preprint doi: https://doi.org/10.1101/2025.09.24.678321; this version posted September 26, 2025. The copyright holder for this preprint (which was not certified by peer review) is the author/funder, who has granted bioRxiv a license to display the preprint in perpetuity. It is made available under a CC-BY 4.0 International license.

53. Botha, D. *et al.* Soil type and precipitation level have a greater influence on fungal than bacterial diversity in serpentine and non-serpentine biological soil crusts. *Ecological Research* **39**, 862–878 (2024).

54. Escola Oliva, G. *et al.* Rhizosphere microbiome and plant growth promotion bacteria isolates enhance salinity tolerance in salt-sensitive Brassica fruticulosa. (2025) doi:10.22541/au.174124680.05965302/v1.

55. Cao, Y. *et al.* microbiomeMarker: an R/Bioconductor package for microbiome marker identification and visualization. *Bioinformatics* **38**, 4027–4029 (2022).

56. Akbari, A., Gharanjik, S., Koobaz, P. & Sadeghi, A. Plant growth promoting Streptomyces strains are selectively interacting with the wheat cultivars especially in saline conditions. *Heliyon* **6**, (2020).

57. Shepherdson, E. M., Baglio, C. R. & Elliot, M. A. Streptomyces behavior and competition in the natural environment. *Current Opinion in Microbiology* **71**, 102257 (2023).

58. Zhang, C. *et al.* Phosphoribosylpyrophosphate synthetase as a metabolic valve advances Methylobacterium/Methylorubrum phyllosphere colonization and plant growth. *Nat Commun* **15**, 5969 (2024).

59. Weiß, M. *et al.* Sebacinales Everywhere: Previously Overlooked Ubiquitous Fungal Endophytes. *PLoS ONE* **6**, e16793 (2011).

60. Visagie, C. M. *et al.* Identification and nomenclature of the genus *Penicillium*. *Studies in Mycology* **78**, 343–371 (2014).

61. Lu, X., Cao, T., Nguyễn, T. T. T. & Yuan, H.-S. Six New Species of Tomentella (Thelephorales, Basidiomycota) From Tropical Pine Forests in Central Vietnam. *Front. Microbiol.* **13**, 864198 (2022).

62. Yang, J. *et al.* Unveiling the Bioactive Compounds and Therapeutic Potential of Russula: A Comprehensive Review. *JoF* **11**, 341 (2025).

bioRxiv preprint doi: https://doi.org/10.1101/2025.09.24.678321; this version posted September 26, 2025. The copyright holder for this preprint (which was not certified by peer review) is the author/funder, who has granted bioRxiv a license to display the preprint in perpetuity. It is made available under a CC-BY 4.0 International license.

63. Schechter, S. P. & Bruns, T. D. Edaphic sorting drives arbuscular mycorrhizal fungal community assembly in a serpentine/non-serpentine mosaic landscape. *Ecosphere* **3**, art42 (2012).

64. Asif, A., Koner, S., Hussain, B. & Hsu, B.-M. Root-associated functional microbiome endemism facilitates heavy metal resilience and nutrient poor adaptation in native plants under serpentine driven edaphic challenges. *Journal of Environmental Management* **373**, 123826 (2025).

65. Anderson, H. M. *et al.* Root exudation and rhizosphere microbial assembly are influenced by novel plant trait diversity in carrot genotypes. *Soil Biology and Biochemistry* **197**, 109516 (2024).

66. Quiza, L. *et al.* The effect of wheat genotype on the microbiome is more evident in roots and varies through time. *ISME COMMUN.* **3**, 32 (2023).

67. Yang, P., Zhu, X. & Ning, K. Microbiome-based enrichment pattern mining has enabled a deeper understanding of the biome–species–function relationship. *Commun Biol* **6**, 391 (2023).

68. Compant, S., Samad, A., Faist, H. & Sessitsch, A. A review on the plant microbiome: Ecology, functions, and emerging trends in microbial application. *Journal of Advanced Research* **19**, 29–37 (2019).

69. Bollmann-Giolai, A. *et al.* A low-cost pipeline for soil microbiome profiling. *Microbiologyopen* **9**, e1133 (2020).

70. Bilal, S. *et al.* Endophytic Paecilomyces formosus LHL10 Augments Glycine max L. Adaptation to Ni-Contamination through Affecting Endogenous Phytohormones and Oxidative Stress. *Front. Plant Sci.* **8**, 870 (2017).

71. Surono & Narisawa, K. The dark septate endophytic fungus Phialocephala fortinii is a potential decomposer of soil organic compounds and a promoter of Asparagus officinalis growth. *Fungal Ecology* **28**, 1–10 (2017).

72. Branco, S. & Ree, R. H. Serpentine Soils Do Not Limit Mycorrhizal Fungal Diversity. *PLOS ONE* **5**, e11757 (2010).

bioRxiv preprint doi: https://doi.org/10.1101/2025.09.24.678321; this version posted September 26, 2025. The copyright holder for this preprint (which was not certified by peer review) is the author/funder, who has granted bioRxiv a license to display the preprint in perpetuity. It is made available under a CC-BY 4.0 International license.

686 73. Panaccione, D. G., Sheets, N. L., Miller, S. P. & Cumming, J. R. Diversity of Cenococcum
687 geophilum isolates from serpentine and non-serpentine soils. *Mycologia* **93**, 645–652 (2001).
688 74. Santoyo, G. How plants recruit their microbiome? New insights into beneficial interactions.
689 *Journal of Advanced Research* **40**, 45–58 (2022).
690 75. Oyserman, B. O. *et al.* Extracting the GEMs: Genotype, Environment, and Microbiome
691 Interactions Shaping Host Phenotypes. *Front. Microbiol.* **11**, (2021).
692 76. Petersen, C. *et al.* Host and microbiome jointly contribute to environmental adaptation. *ISME J*
693 **17**, 1953–1965 (2023).
694 77. Bhar, A., Chakraborty, A. & Roy, A. The captivating role of calcium in plant-microbe interaction.
695 *Front. Plant Sci.* **14**, 1138252 (2023).
696 78. Coleman-Derr, D. & Tringe, S. G. Building the crops of tomorrow: advantages of symbiont-
697 based approaches to improving abiotic stress tolerance. *Front. Microbiol.* **5**, (2014).
698 79. Bollmann-Giolai, A., Malone, J. G. & Arora, S. Diversity, detection and exploitation: linking soil
699 fungi and plant disease. *Current Opinion in Microbiology* **70**, 102199 (2022).
700 80. Dombrowski, N. *et al.* Root microbiota dynamics of perennial Arabis alpina are dependent on
701 soil residence time but independent of flowering time., Root microbiota dynamics of perennial
702 Arabis alpina are dependent on soil residence time but independent of flowering time. *ISME J*
703 **11, 11**, 43, 43–55 (2017).
704 81. Copeland, J. K., Yuan, L., Layeghifard, M., Wang, P. W. & Guttman, D. S. Seasonal Community
705 Succession of the Phyllosphere Microbiome. *MPMI* **28**, 274–285 (2015).
706 82. Danku, J. M. C., Lahner, B., Yakubova, E. & Salt, D. E. Large-Scale Plant Ionomics. in *Plant*
707 *Mineral Nutrients: Methods and Protocols* (ed. Maathuis, F. J. M.) 255–276 (Humana Press,
708 Totowa, NJ, 2013). doi:10.1007/978-1-62703-152-3_17.
709 83. Ginestet, C. ggplot2: Elegant Graphics for Data Analysis. *Journal of the Royal Statistical Society:*
710 *Series A (Statistics in Society)* **174**, 245–246 (2011).

bioRxiv preprint doi: https://doi.org/10.1101/2025.09.24.678321; this version posted September 26, 2025. The copyright holder for this preprint (which was not certified by peer review) is the author/funder, who has granted bioRxiv a license to display the preprint in perpetuity. It is made available under a CC-BY 4.0 International license.

711 84. Kassambara, A. ggpubr: 'ggplot2' Based Publication Ready Plots. 0.6.1
712 https://doi.org/10.32614/CRAN.package.ggpubr (2016).
713 85. Kassambara, A. & Mundt, F. factoextra: Extract and Visualize the Results of Multivariate Data
714 Analyses. 1.0.7 https://doi.org/10.32614/CRAN.package.factoextra (2016).
715 86. Massicotte, P. & South, A. rnaturalearth: World Map Data from Natural Earth. 1.1.0
716 https://doi.org/10.32614/CRAN.package.rnaturalearth (2017).
717 87. Bulgarelli, D. *et al.* Revealing structure and assembly cues for Arabidopsis root-inhabiting
718 bacterial microbiota. *Nature* **488**, 91–95 (2012).
719 88. Bodenhausen, N., Horton, M. W. & Bergelson, J. Bacterial communities associated with the
720 leaves and the roots of Arabidopsis thaliana. *PLoS ONE* **8**, e56329 (2013).
721 89. Horton, M. W. *et al.* Genome-wide association study of Arabidopsis thaliana leaf microbial
722 community. *Nat Commun* **5**, 5320 (2014).
723 90. Qvit-Raz, N., Jurkevitch, E. & Belkin, S. Drop-size soda lakes: transient microbial habitats on a
724 salt-secreting desert tree. *Genetics* **178**, 1615–1622 (2008).
725 91. Walters, W. *et al.* Improved Bacterial 16S rRNA Gene (V4 and V4-5) and Fungal Internal
726 Transcribed Spacer Marker Gene Primers for Microbial Community Surveys. *mSystems* **1**,
727 e00009-15 (2016).
728 92. Lundberg, D. S., Yourstone, S., Mieczkowski, P., Jones, C. D. & Dangl, J. L. Practical innovations
729 for high-throughput amplicon sequencing. *Nat Meth* **10**, 999–1002 (2013).
730 93. Martin, M. Cutadapt removes adapter sequences from high-throughput sequencing reads.
731 *EMBnet.journal* **17**, 10–12 (2011).
732 94. Chen, S., Zhou, Y., Chen, Y. & Gu, J. fastp: an ultra-fast all-in-one FASTQ preprocessor.
733 *Bioinformatics* **34**, i884–i890 (2018).
734 95. Callahan, B. J., Sankaran, K., Fukuyama, J. A., McMurdie, P. J. & Holmes, S. P. Bioconductor
735 Workflow for Microbiome Data Analysis: from raw reads to community analyses.
736 *F1000Research* **5**, 1492 (2016).

bioRxiv preprint doi: https://doi.org/10.1101/2025.09.24.678321; this version posted September 26, 2025. The copyright holder for this preprint (which was not certified by peer review) is the author/funder, who has granted bioRxiv a license to display the preprint in perpetuity. It is made available under a CC-BY 4.0 International license.

96. Quast, C. *et al.* The SILVA ribosomal RNA gene database project: improved data processing and web-based tools. *Nucleic Acids Res* **41**, D590–D596 (2013).

97. Nilsson, R. H. *et al.* The UNITE database for molecular identification of fungi: handling dark taxa and parallel taxonomic classifications. *Nucleic Acids Res* **47**, D259–D264 (2019).

98. McMurdie, P. J. & Holmes, S. phyloseq: An R Package for Reproducible Interactive Analysis and Graphics of Microbiome Census Data. *PLOS ONE* **8**, e61217 (2013).

99. Dixon, P. VEGAN, a package of R functions for community ecology. *Journal of Vegetation Science* **14**, 927–930 (2003).

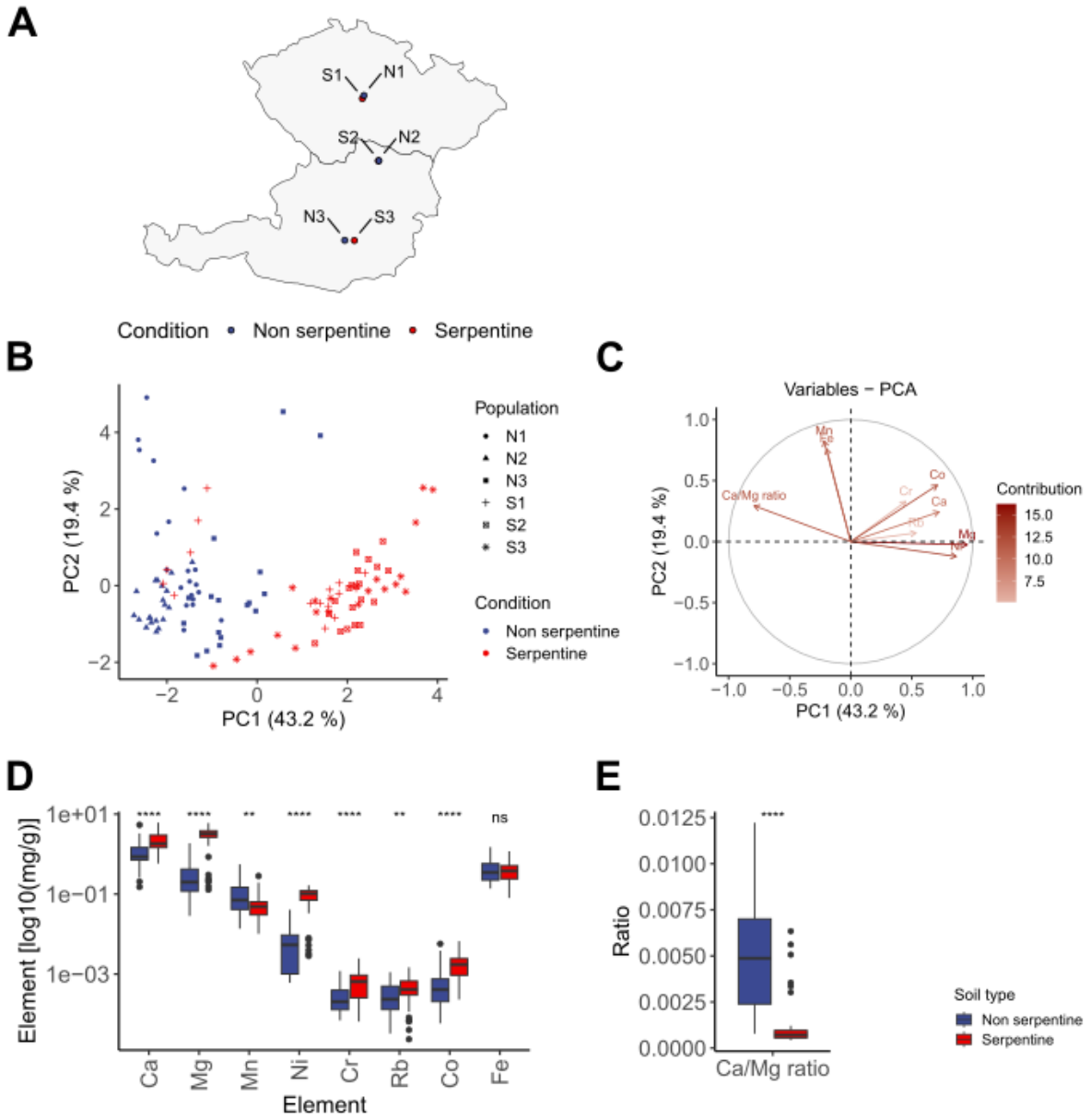
100. Murray, K. D., Webers, C., Ong, C. S., Borevitz, J. & Warthmann, N. kWIP: The k-mer weighted inner product, a de novo estimator of genetic similarity. *PLoS Comput Biol* **13**, e1005727 (2017).

101. Bates, D., Maechler, M., Bolker, B. & Walker, S. lme4: Linear Mixed-Effects Models using 'Eigen' and S4. 1.1-37 https://doi.org/10.32614/CRAN.package.lme4 (2003).

102. Lüdecke, D. *et al.* performance: Assessment of Regression Models Performance. 0.15.0 https://doi.org/10.32614/CRAN.package.performance (2019).

bioRxiv preprint doi: https://doi.org/10.1101/2025.09.24.678321; this version posted September 26, 2025. The copyright holder for this preprint (which was not certified by peer review) is the author/funder, who has granted bioRxiv a license to display the preprint in perpetuity. It is made available under a CC-BY 4.0 International license.

754 **Figures**



755

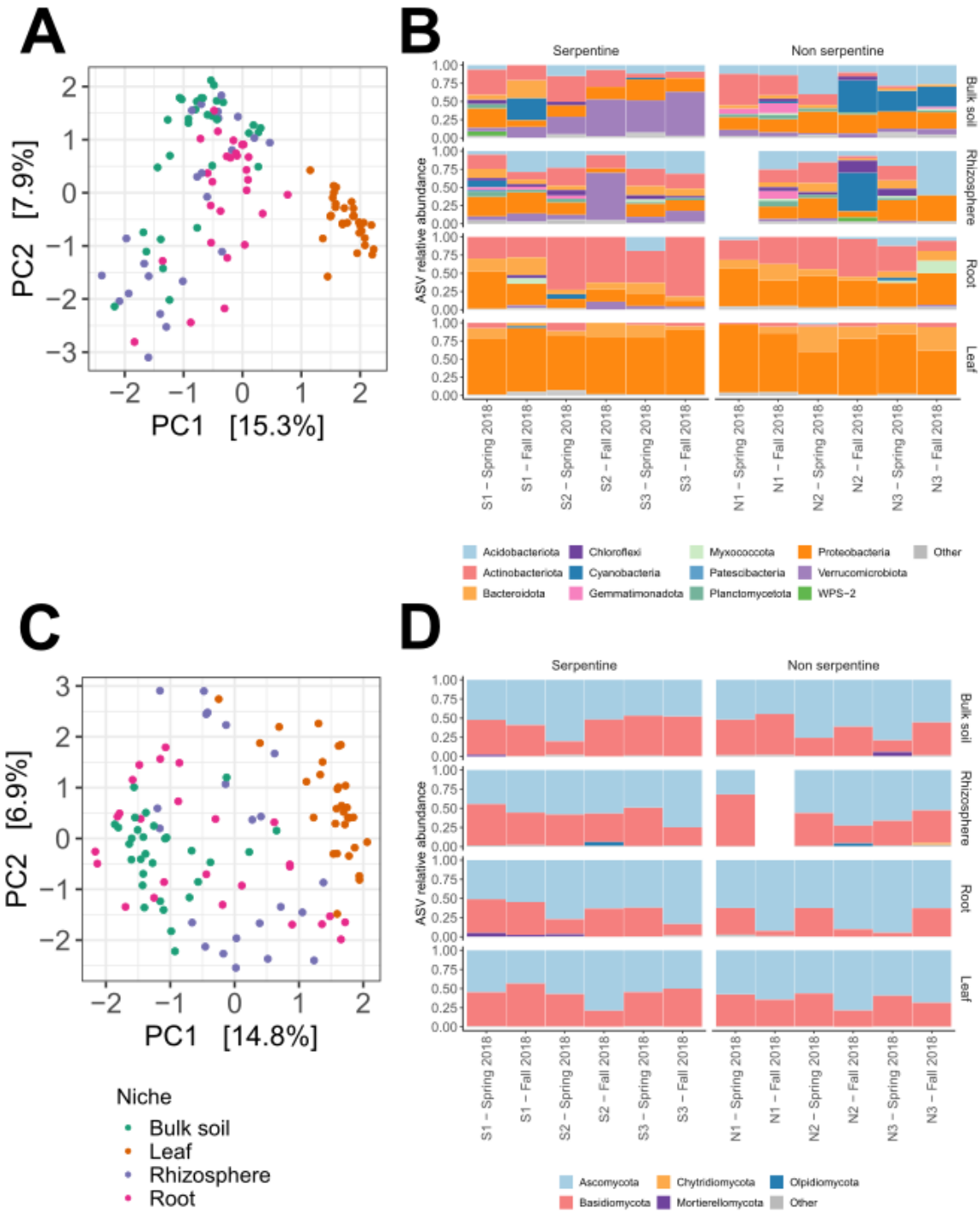
756 **Fig. 1 Serpentine soils, and their associated *A. arenosa* populations, display elevated metal ion**
757 **concentrations and a lower calcium to magnesium ratio than non-serpentine samples. (A)**
758 Geographical locations of serpentine and non-serpentine populations in Austria and the Czech
759 Republic. **(B)** PCA of soil ion composition showing clear separation of serpentine and non-serpentine
760 sites. **(C)** PCA biplot illustrating contributions of individual ions and the Ca/Mg ratio to the first two
761 principal components. **(D)** Ion concentrations obtained from soil profiling. Labels indicate statistically
762 significant differences between serpentine and non-serpentine soils (t-test).
763 **(E)** Difference in Ca/Mg ratio between serpentine and non-serpentine soils (t-test). ($p < 0.0001$****, p
764 < 0.001***, $p < 0.01$**, $p < 0.05$*; not significant: ns)

765

766

767

bioRxiv preprint doi: https://doi.org/10.1101/2025.09.24.678321; this version posted September 26, 2025. The copyright holder for this preprint (which was not certified by peer review) is the author/funder, who has granted bioRxiv a license to display the preprint in perpetuity. It is made available under a CC-BY 4.0 International license.



768

769 **Fig. 2 Higher bacterial variation in below-ground niches and higher uniformity for fungal**
770 **communities across all niches. (A)** RDA of bacterial communities in bulk soil, rhizosphere, root, and
771 leaf niches. **(B)** Relative abundance of bacterial phyla across all populations and seasons (spring and
772 fall 2018). **(C)** RDA of fungal communities in bulk soil, rhizosphere, root, and leaf niches. **(D)** Relative
773 abundance of fungal phyla across all populations and seasons (spring and fall 2018). Fall 2018 was used
774 as representative season for A and C. (Phyla with a total relative abundance of less than 2 % were
775 grouped as 'Other'.)

776

bioRxiv preprint doi: https://doi.org/10.1101/2025.09.24.678321; this version posted September 26, 2025. The copyright holder for this preprint (which was not certified by peer review) is the author/funder, who has granted bioRxiv a license to display the preprint in perpetuity. It is made available under a CC-BY 4.0 International license.

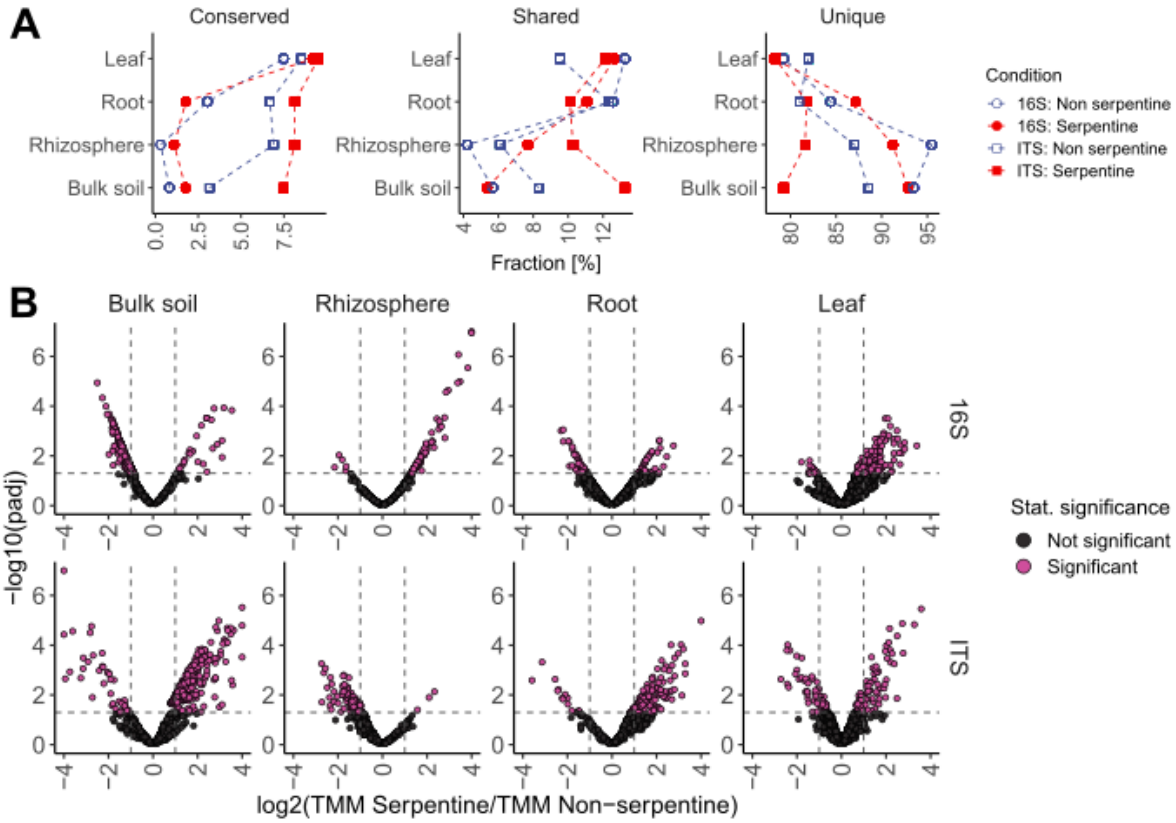


Fig. 3 Similarity of bacterial and fungal microbiomes across plant populations based on ASV presence-absence and differential enrichment. (A) Distribution of bacterial and fungal ASVs across niches, categorised as conserved (present in all three populations), shared (present in two populations), or unique (restricted to a single population). Fungal ASVs were more conserved than bacterial ASVs under both serpentine and non-serpentine conditions. **(B)** Differential abundance of conserved bacterial and fungal ASVs between serpentine and non-serpentine soils. Volcano plots show significantly enriched ASVs.

bioRxiv preprint doi: https://doi.org/10.1101/2025.09.24.678321; this version posted September 26, 2025. The copyright holder for this preprint (which was not certified by peer review) is the author/funder, who has granted bioRxiv a license to display the preprint in perpetuity. It is made available under a CC-BY 4.0 International license.

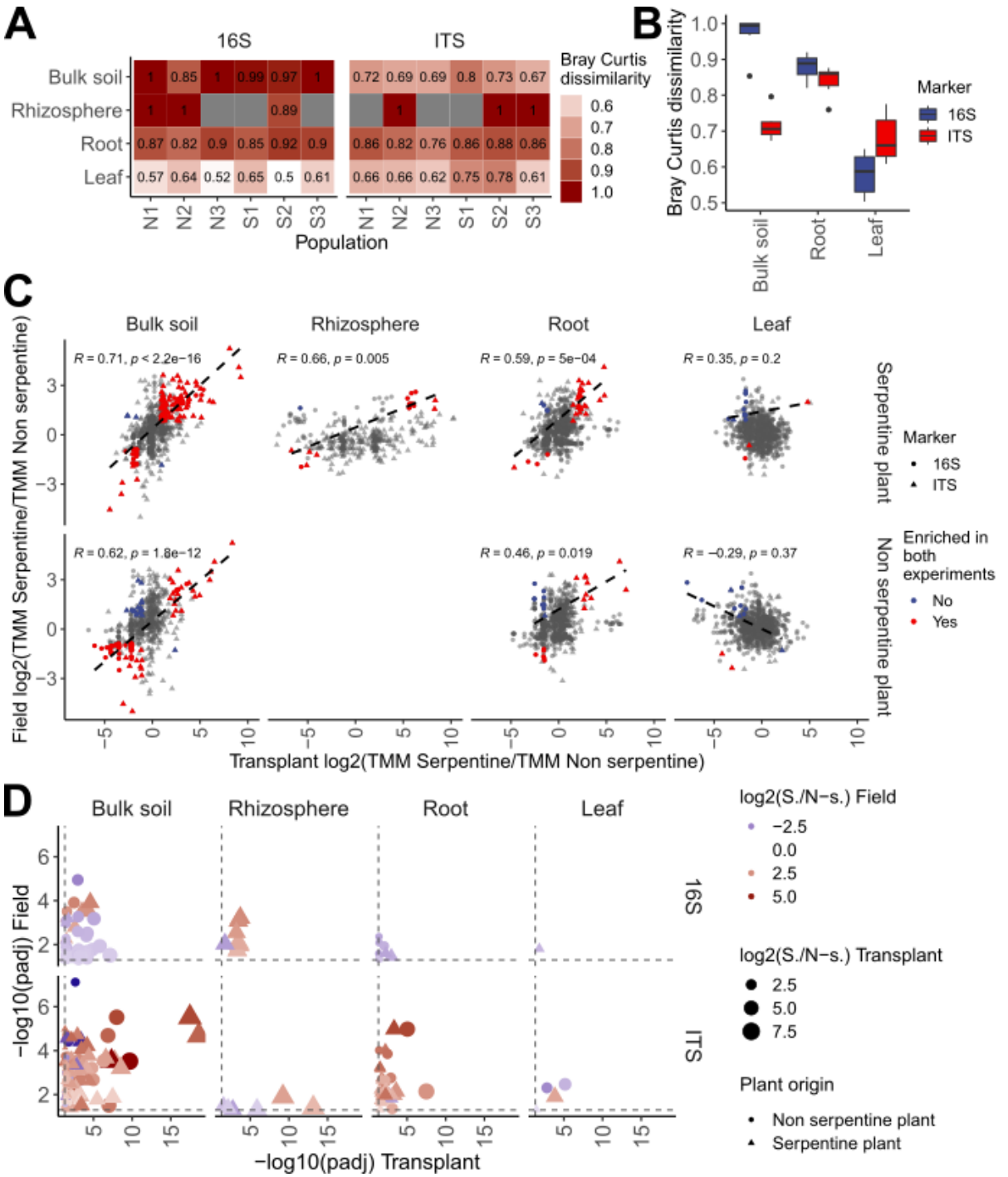


Fig. 4 Microbiome responses in a reciprocal transplant experiment. (A,B) Bray-Curtis dissimilarity shows that microbiomes of transplanted plants differ from, but partially retain, those in native soils, with fungi showing greater similarity across compartments than bacteria. The heatmap in **(A)** shows Bray-Curtis dissimilarity scores per population and niche for bacteria and fungi, boxplot **(B)** visualises the Bray-Curtis dissimilarity scores next to one another across niches. **(C)** Spearman correlations of log2 fold-changes reveal that serpentine plants more closely mirror field enrichment patterns than non-serpentine plants, particularly belowground. **(D)** Differential abundance analysis identifies ASVs enriched in serpentine versus non-serpentine soils, with overlap to field-enriched ASVs highlighting candidates potentially contributing to serpentine adaptation.

bioRxiv preprint doi: https://doi.org/10.1101/2025.09.24.678321; this version posted September 26, 2025. The copyright holder for this preprint (which was not certified by peer review) is the author/funder, who has granted bioRxiv a license to display the preprint in perpetuity. It is made available under a CC-BY 4.0 International license.

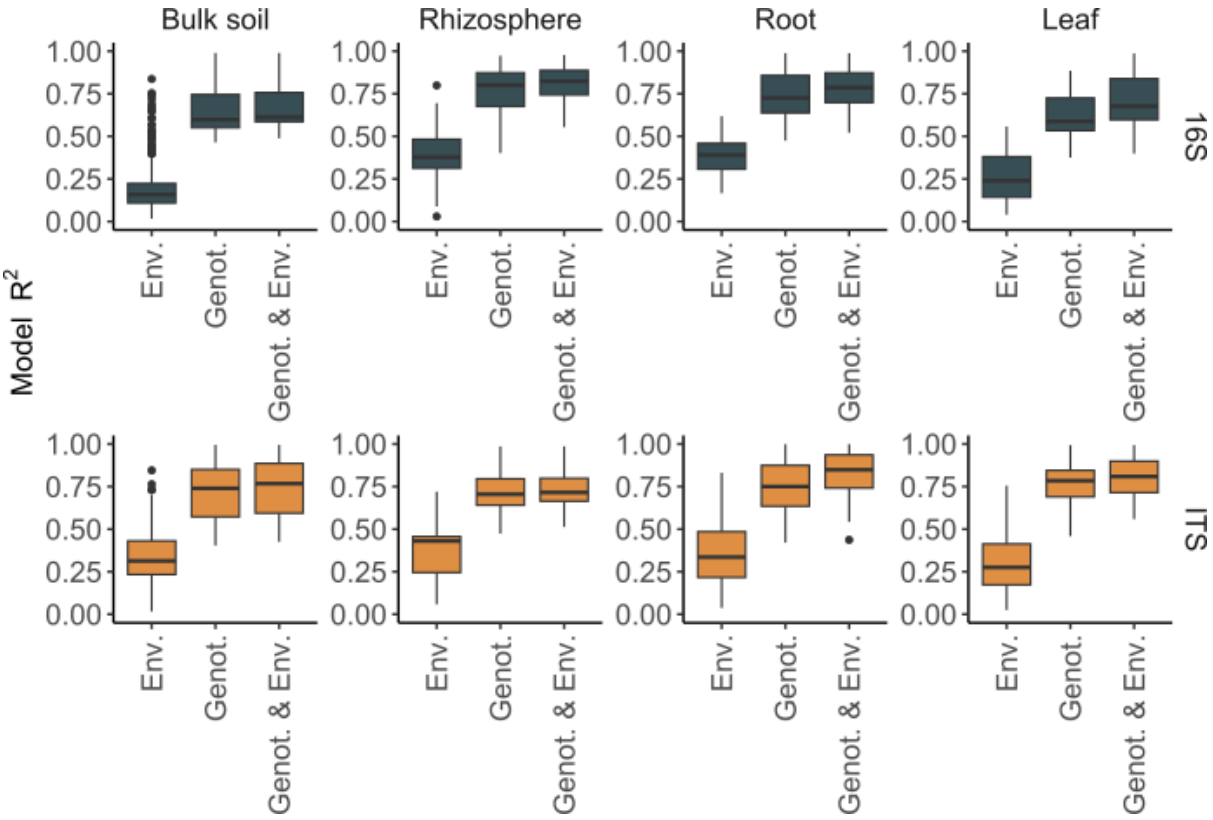


Fig. 5 Contributions of genotype and environment to microbiome composition. Explained variance (R^2) of ASV abundance is shown for statistically significant models predicting ASV relative abundance, with genotype and environment as fixed factors and time as a random factor. While the combination of genotype and environment best predicts ASV abundance, genetic effects consistently exceed environmental effects in shaping microbiome assembly.

bioRxiv preprint doi: https://doi.org/10.1101/2025.09.24.678321; this version posted September 26, 2025. The copyright holder for this preprint (which was not certified by peer review) is the author/funder, who has granted bioRxiv a license to display the preprint in perpetuity. It is made available under a CC-BY 4.0 International license.

Additional Files

Extended Data File 1: Statistical analysis of ion compositions in serpentine and non-serpentine soils.

Extended Data File 2: Word document containing supplementary figures, alpha- and beta-diversity analyses.

Extended Data File 3: Percentages of bacterial and fungal phyla detected across seasons, populations, and niches.

Extended Data File 4: Percentages of conserved, shared, and unique fungal and bacterial ASVs across populations.

Extended Data File 5: Table displaying percentages of bacterial and fungal ASVs enriched in serpentine and non-serpentine soils.

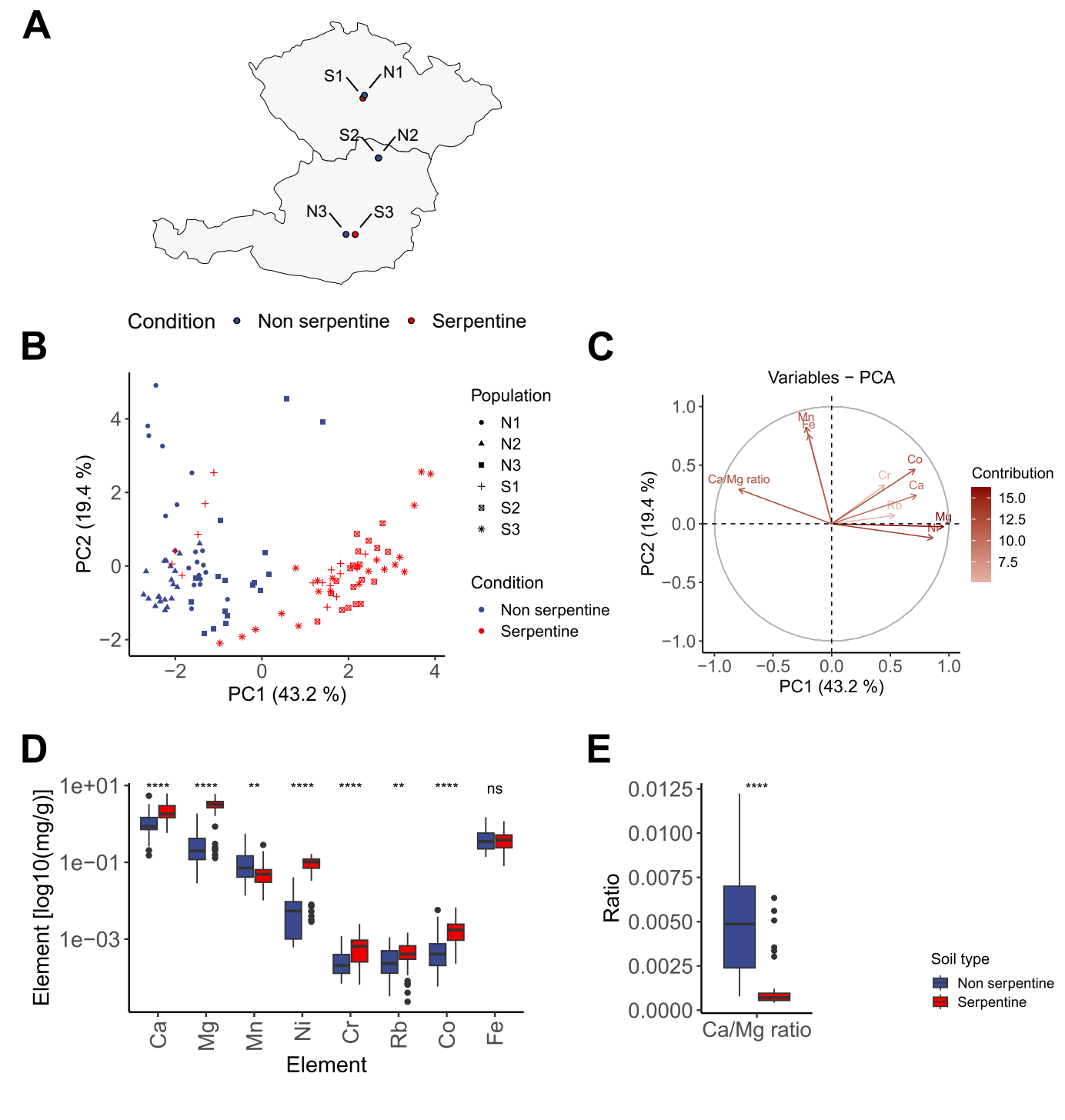
Extended Data File 6: Results from field enrichment testing.

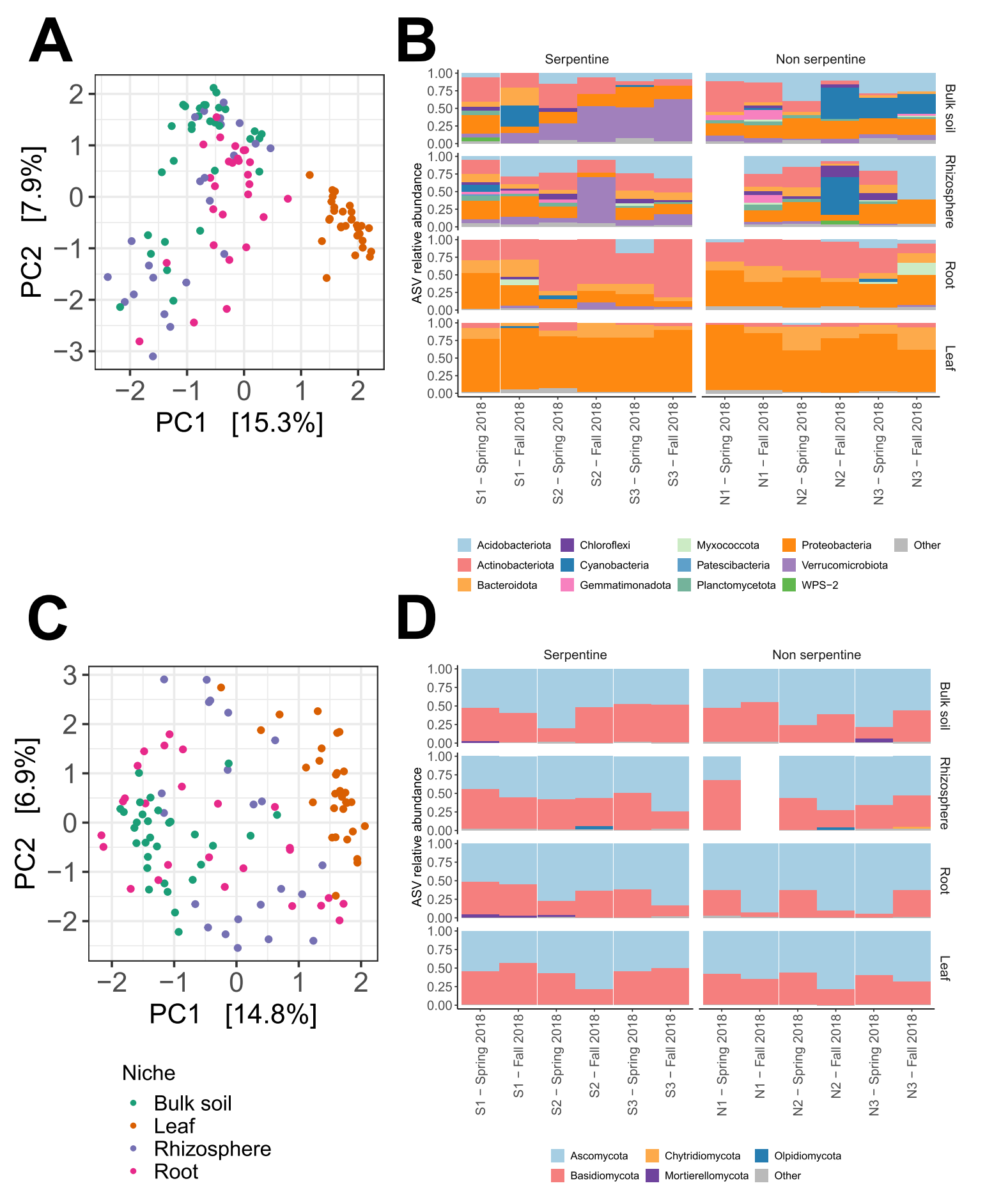
Extended Data File 7: ASVs per genus from the field enrichment experiment.

Extended Data File 8: Comparison of transplant and field enrichment testing results.

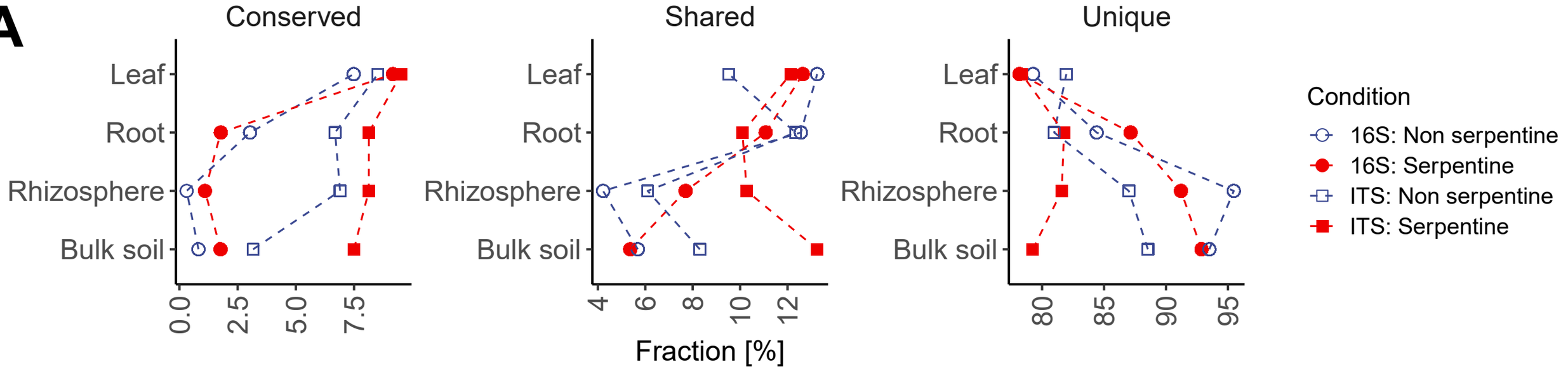
Extended Data File 9: Overlap of enrichment testing for serpentine-enriched bacterial and fungal ASVs between field and transplant.

Extended Data File 10: Excel file containing sequencing adapters, barcodes, and primers.

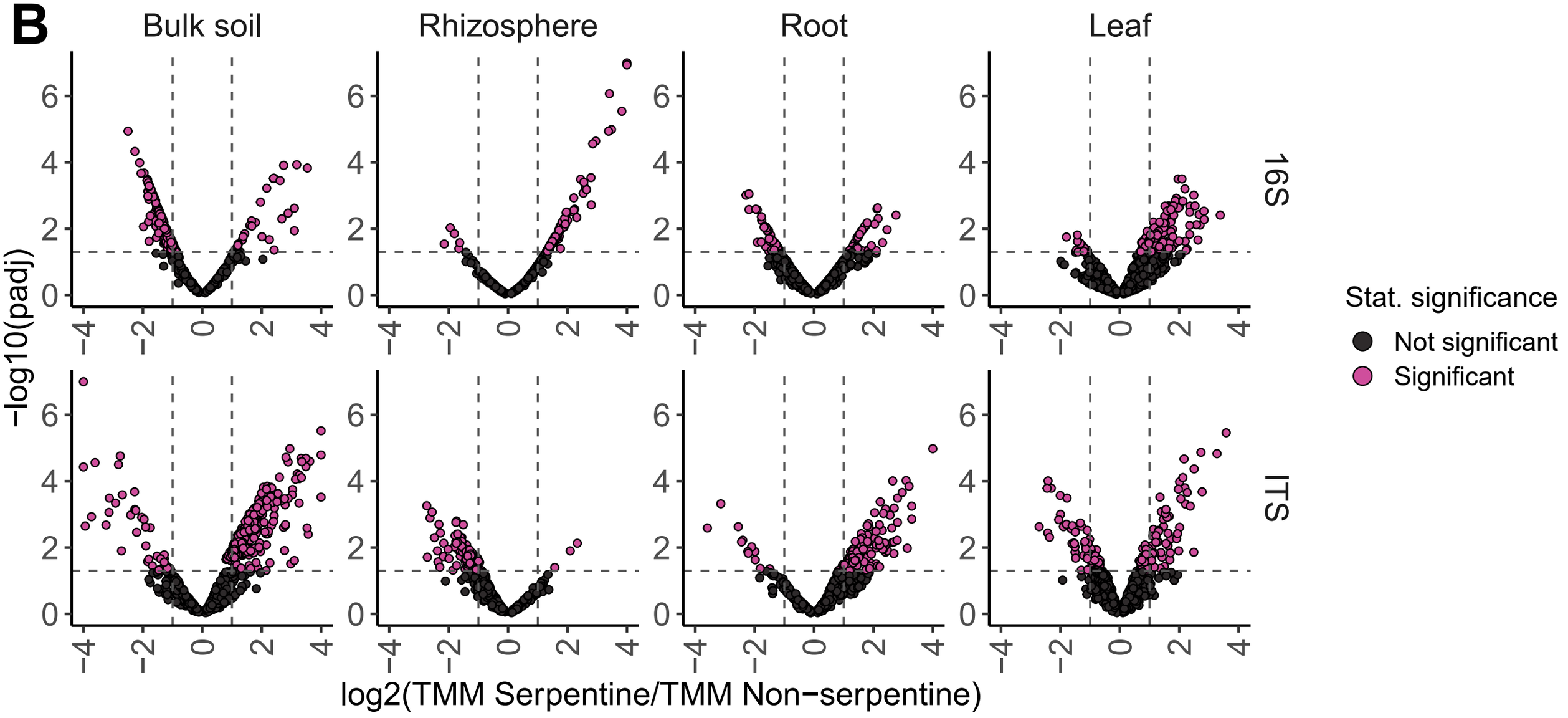

A
S1
N1
S2
N2
N3
S3
Condition
Non serpentine
Serpentine
B
PC2 (19.4 %)
PC1 (43.2 %)
Population
N1
N2
N3
S1
S2
S3
Condition
Non serpentine
Serpentine
C
Variables − PCA
PC2 (19.4 %)
PC1 (43.2 %)
Mn
Fe
Co
Cr
Ca
Rb
Mg
Ni
Ca/Mg ratio
Contribution
15.0
12.5
10.0
7.5
D
Element [log10(mg/g)]
1e+01
1e−01
1e−03
****
****
**
****
****
**
****
ns
Ca
Mg
Mn
Ni
Cr
Rb
Co
Fe
Element
E
Ratio
0.0125
0.0100
0.0075
0.0050
0.0025
0.0000
****
Ca/Mg ratio
Soil type
Non serpentine
Serpentine

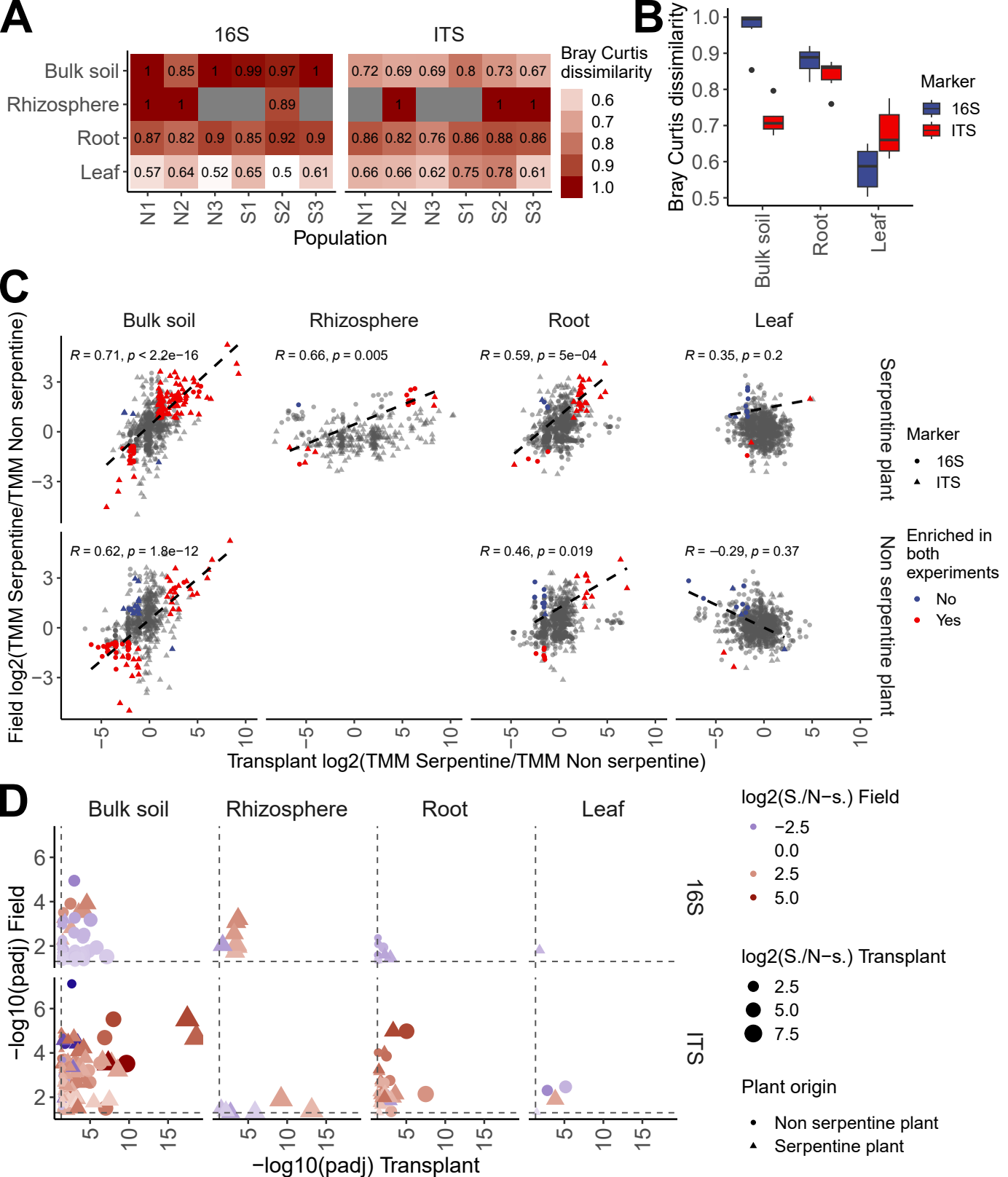

A
PC2 [7.9%]
PC1 [15.3%]
B
Serpentine
Non serpentine
Bulk soil
Rhizosphere
Root
Leaf
ASV relative abundance
S1 – Spring 2018
S1 – Fall 2018
S2 – Spring 2018
S2 – Fall 2018
S3 – Spring 2018
S3 – Fall 2018
N1 – Spring 2018
N1 – Fall 2018
N2 – Spring 2018
N2 – Fall 2018
N3 – Spring 2018
N3 – Fall 2018
Acidobacteriota
Actinobacteriota
Bacteroidota
Chloroflexi
Cyanobacteria
Gemmatimonadota
Myxococcota
Patescibacteria
Planctomycetota
Proteobacteria
Verrucomicrobiota
WPS−2
Other
C
PC2 [6.9%]
PC1 [14.8%]
Niche
Bulk soil
Leaf
Rhizosphere
Root
D
Serpentine
Non serpentine
Bulk soil
Rhizosphere
Root
Leaf
ASV relative abundance
Ascomycota
Basidiomycota
Chytridiomycota
Mortierellomycota
Olpidiomycota
Other

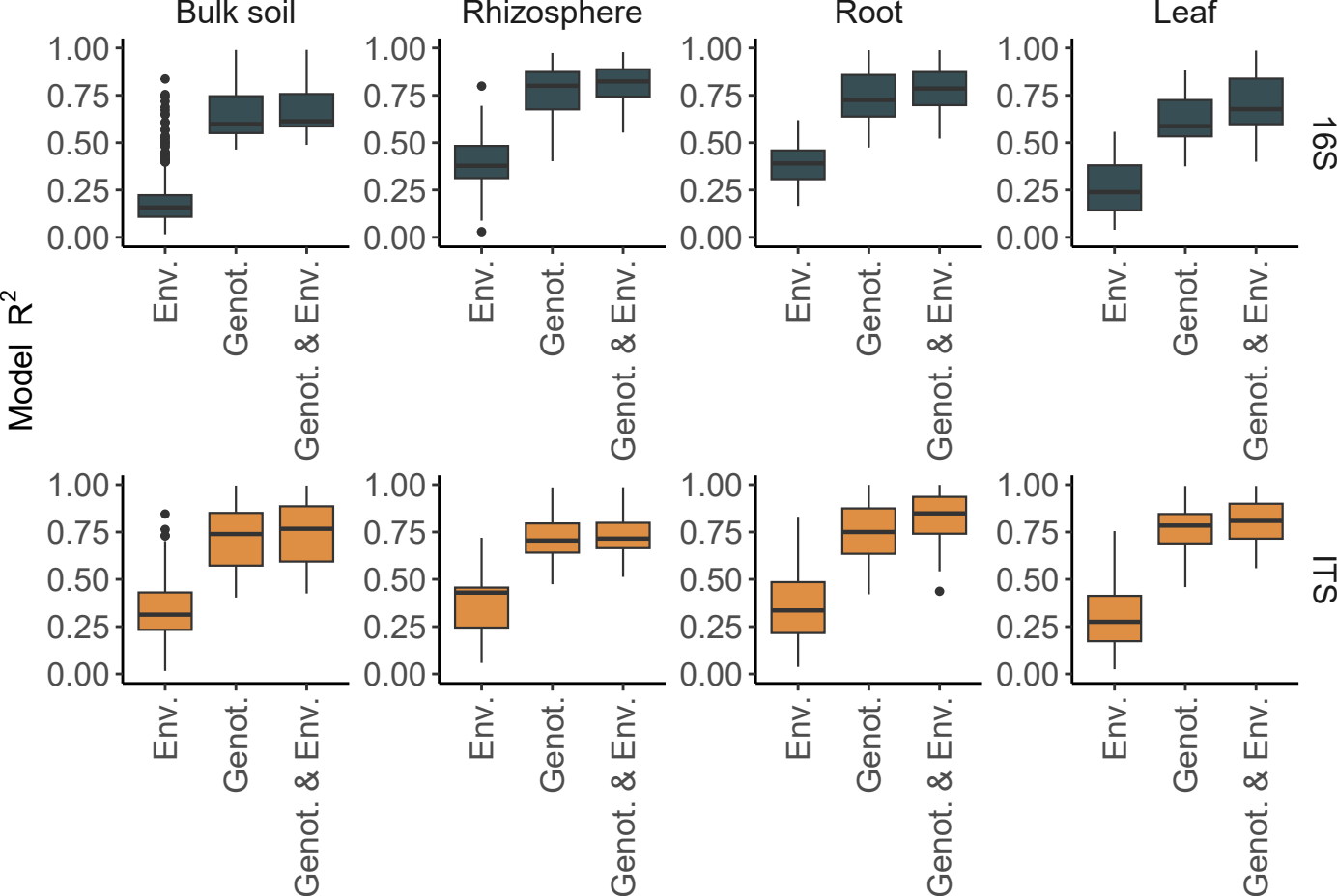
A


Conserved
Shared
Unique
Leaf
Root
Rhizosphere
Bulk soil
0.0
2.5
5.0
7.5
4
6
8
10
12
80
85
90
95
Fraction [%]
Condition
16S: Non serpentine
16S: Serpentine
ITS: Non serpentine
ITS: Serpentine

B


Bulk soil
Rhizosphere
Root
Leaf
16S
ITS
−log10(padj)
log2(TMM Serpentine/TMM Non−serpentine)
Stat. significance
Not significant
Significant


A
16S
ITS
Bulk soil
Rhizosphere
Root
Leaf
1 0.85 1 0.99 0.97 1
1 1 0.89
0.87 0.82 0.9 0.85 0.92 0.9
0.57 0.64 0.52 0.65 0.5 0.61
0.72 0.69 0.69 0.8 0.73 0.67
1 1 1
0.86 0.82 0.76 0.86 0.88 0.86
0.66 0.66 0.62 0.75 0.78 0.61
N1 N2 N3 S1 S2 S3
Population
Bray Curtis dissimilarity
0.6
0.7
0.8
0.9
1.0
B
Bray Curtis dissimilarity
1.0
0.9
0.8
0.7
0.6
0.5
Bulk soil
Root
Leaf
Marker
16S
ITS
C
Bulk soil
Rhizosphere
Root
Leaf
R = 0.71, p < 2.2e−16
R = 0.66, p = 0.005
R = 0.59, p = 5e−04
R = 0.35, p = 0.2
R = 0.62, p = 1.8e−12
R = 0.46, p = 0.019
R = −0.29, p = 0.37
Field log2(TMM Serpentine/TMM Non serpentine)
Transplant log2(TMM Serpentine/TMM Non serpentine)
Serpentine plant
Non serpentine plant
Marker
16S
ITS
Enriched in both experiments
No
Yes
D
Bulk soil
Rhizosphere
Root
Leaf
16S
ITS
−log10(padj) Field
−log10(padj) Transplant
log2(S./N−s.) Field
−2.5
0.0
2.5
5.0
log2(S./N−s.) Transplant
2.5
5.0
7.5
Plant origin
Non serpentine plant
Serpentine plant


Bulk soil
Rhizosphere
Root
Leaf
16S
ITS
Model R2
1.00
0.75
0.50
0.25
0.00
Env.
Genot.
Genot. & Env.